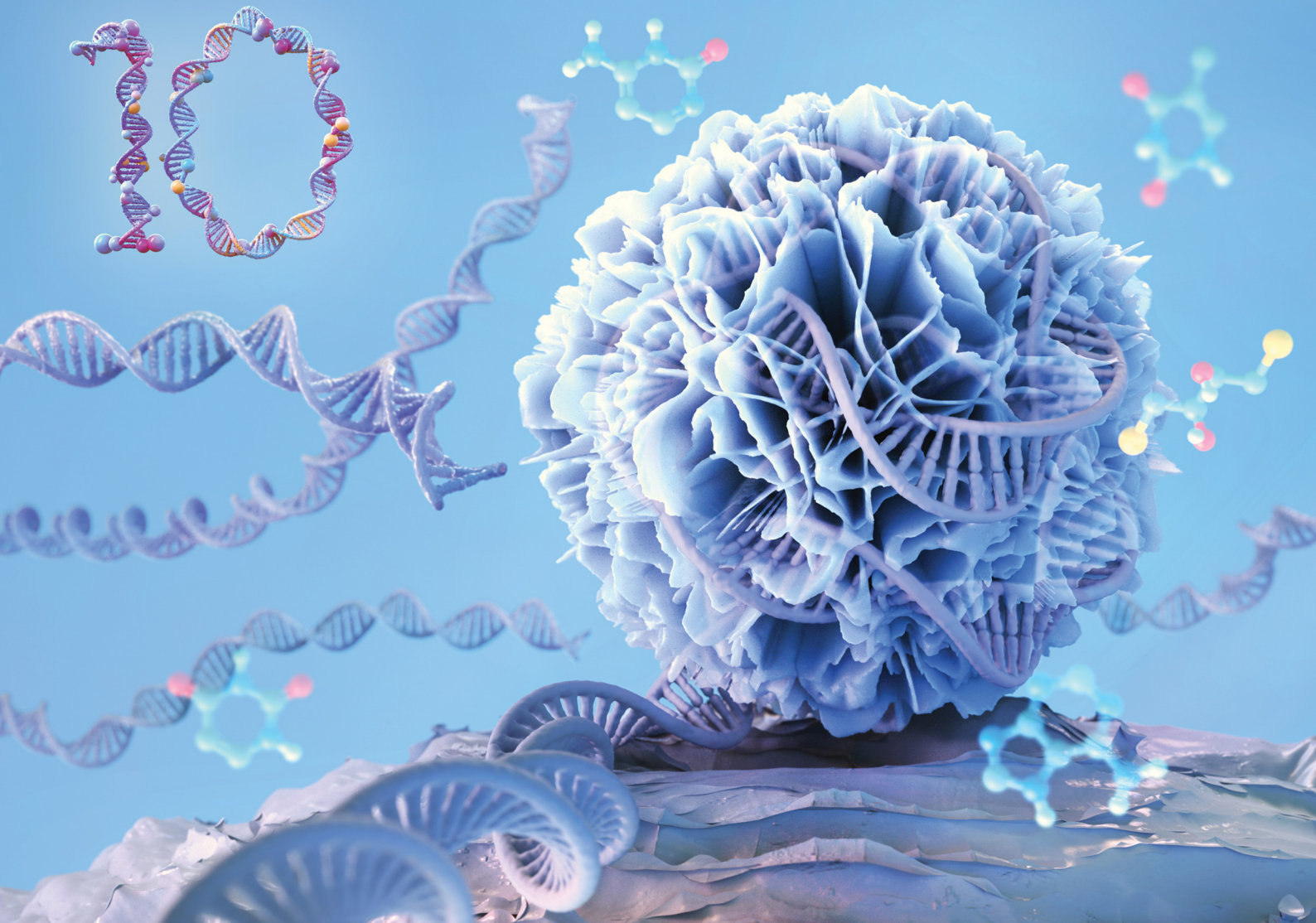


Volume 10
Number 12
December 2025
Pages 3129–3508

Nanoscale Horizons

The home for rapid reports of exceptional significance in nanoscience and nanotechnology
rsc.li/nanoscale-horizons



ISSN 2055-6756



MINIREVIEW

Young Hoon Roh *et al.*

Rolling circle replication based nucleic acid nanostructures
for programmable drug delivery





Cite this: *Nanoscale Horiz.*, 2025,
10, 3290

Rolling circle replication based nucleic acid nanostructures for programmable drug delivery

Kyungjik Yang, Keonwook Nam, Kyung Hoon Park, Hae Kyung Shin, Yeongmok Kim and Young Hoon Roh *

Nucleic acid nanostructures are powerful nanomaterials for biomedical applications owing to their inherent programmability, biocompatibility, and biodegradability. However, their usability has been limited by inefficient synthesis methods and their susceptibility to degradation in physiological environments. To overcome these challenges, rolling circle replication (RCR), an isothermal enzymatic reaction, has emerged as a polymerization method to generate ultra-long nucleic acid nanostructures with improved productivity, biostability, and functionality. This minireview provides a general overview of the versatile biological functions and engineering strategies for RCR based nucleic acid nanostructures. We also highlight recent advances in passive targeted delivery, active targeted delivery, and stimulus responsive delivery using polymeric DNA and RNA nanostructures. Finally, we outline the current status, key challenges, and future perspectives of nucleic acid nanostructures for advanced drug delivery.

Received 30th April 2025,
Accepted 12th September 2025

DOI: 10.1039/d5nh00293a

rsc.li/nanoscale-horizons

1. Introduction

The nucleic acids, deoxyribonucleic acid (DNA) and ribonucleic acid (RNA), are biocompatible macromolecules found in all living organisms that play a fundamental role in the storage and transfer of genetic information.¹ In addition to their canonical roles, nucleic acids facilitate various biological functions and are capable of forming nanostructures *via* sequence

design.^{2,3} Further, the flexibility, programmability, and spatial addressability of nucleic acid nanostructures can be controlled using Watson–Crick base pairing. Various nucleic acid nanostructures such as nucleic acid tetrahedrons, nucleic acid origami, branched nucleic acid nanostructures, polymeric nucleic acid nanostructures, and spherical nucleic acid nanostructures have been developed using bottom-up assembly, origami assembly, composite material assembly, and rolling circle replication (RCR).^{4–6} Due to their high biocompatibility, programmable structures, and chemical modification, these nanostructures have been utilized in various biomedical applications including drug delivery, biosensing, and bioimaging.

Department of Biotechnology, College of Life Science and Biotechnology, Yonsei University, 50 Yonsei-ro, Seodaemun-gu, Seoul 03722, South Korea.
E-mail: yr36@yonsei.ac.kr



Kyungjik Yang

mucoadhesive carbohydrate biopolymers for advanced drug delivery.

Kyungjik Yang received his BSc in the Department of Biotechnology from the Catholic University of Korea. He completed his PhD in the Department of Biotechnology under Prof. Young Hoon Roh at Yonsei University. Currently, he works as a postdoctoral fellow at Harvard Medical School. His research interests lie in the fields of nucleic acid nanotechnology, engineering of nanoparticle surfaces and sizes, development of targeting moiety, and design of



Young Hoon Roh

continued success in advancing nanoscience and biomaterials research.

Young Hoon Roh is a professor in the Department of Biotechnology at Yonsei University. His research interests focus on the fields of nucleic acid nanotechnology, biopolymers, and hydrogels for biomedical applications including drug delivery systems. As a contributor to RSC journals and guest editor for the “DNA Nanotechnology” themed collection, he congratulates Nanoscale Horizons on its 10th anniversary and looks forward to its

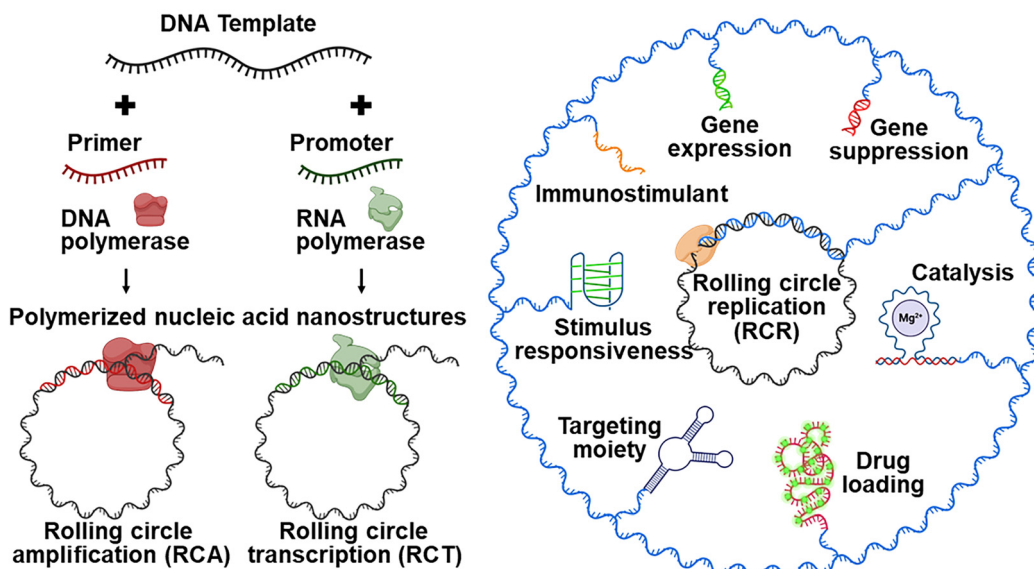


Fig. 1 The schematic for the reaction mechanism and various biological functions of rolling circle replication (RCR). Rolling circle amplification (RCA) and rolling circle transcription (RCT) were performed to synthesize polymerized DNA/RNA nanostructures with DNA template, primer/promoter, DNA/RNA polymerase. The figures were created with BioRender.

Among the methods used for nucleic acid nanostructures generation, RCR, involving isothermal amplification, has emerged as a particularly powerful method for synthesizing ultra-long polymeric nucleic acid nanostructures. Inspired by the circular DNA replication mechanisms found in microorganisms, rolling circle amplification (RCA) was first introduced by Andrew Fire's group in 1995 to generate long single-stranded DNA (ssDNA) from a circular DNA template using DNA polymerase.⁷ In parallel, rolling circle transcription (RCT), introduced by Eric Kool's group the same year, enabled the synthesis of long RNA transcripts by employing RNA polymerase instead.⁸ RCA and RCT reactions for the generation of ultra-long polymeric DNA and RNA, respectively, begin with the preparation of a circular template, which is produced from a linear DNA template and its complementary primer for RCA or promoter for RCT (Fig. 1). The resulting circular DNA template is then amplified using DNA polymerase in RCA or RNA polymerase in RCT. RCR based strategies have enabled the development of multifunctional DNA/RNA nanostructures for programmable drug delivery.^{9–11} By rationally designing circular DNA templates, these structures can be endowed with diverse functions, including gene regulation, immunostimulation, catalysis, targeting, and stimuli responsiveness. Owing to their polymeric form, RCR based nucleic acid nanostructures exhibit significantly enhanced stability, versatility, and biofunctionality compared with that of monomeric nucleic acids.

The physicochemical properties of polymeric nucleic acid nanostructures are crucial for their performance in advanced drug delivery systems.^{12–15} As products of enzymatic reactions, these nanostructures offer high tunability, allowing precise control over their structural features by adjusting the reaction parameters. This controllability can be leveraged to optimize the loading, release, and delivery of drugs for therapeutic

applications. Thus, recent studies have focused on engineering nucleic acid length,^{16–18} size,^{18–21} morphology,^{21–24} and density^{24–27} of RCR based nucleic acid nanostructures. This tunability facilitates the rational design of nanostructures with enhanced biological functions, including prolonged circulation time, targeted delivery, controlled drug release, and efficient endosomal escape.

In this minireview, we summarize the recent advances in RCR based nucleic acid nanostructures and discuss their biological functions, engineering strategies, and programmable drug delivery applications. Finally, we conclude with the current challenges and future perspectives of nucleic acid nanostructures applications in the field of drug delivery.

2. Biological functions

RCR based nucleic acid nanostructures have been employed in various biomedical applications by incorporating biologically functional sequences into template DNA. Polymeric DNA and RNA nanostructures have been extensively used for programmable drug delivery because of their inherent structural and functional advantages. Representative biological functions harnessed using nucleic acid based drug delivery systems include gene regulation, immunostimulation, catalysis, drug loading, targeting specific moieties, and stimulus dynamics (Table 1). In this section, we introduce the biological functions utilized in RCR based drug delivery and highlight cases that leverage the structural and functional advantages of RCR based nucleic acid nanostructures.

2.1. Gene downregulation

Nucleic acid based strategies for the downregulation of genes have emerged as powerful therapeutic modalities for drug

Table 1 Representative biological functions of rolling circle replication based nucleic acid nanostructures

Biological function	Therapeutics	RCR type	Targeted cell	Ref.
Gene downregulation	siRNA (luciferase)	RCT	Ovarian cancer (T22)	29
	siRNA (PLK1)	RCT	Ovarian cancer (SKOV3)	32
	siRNA (BCL2)	RCT	Non-Hodgkin's lymphoma (Daudi, Raji, Ramos, Toledo)	33
	siRNA (PLK1)	RCT	Triple-negative breast cancer (MDA-MB-231)	18
	miRNA (34a)	RCT	Prostate cancer (PC3)	36
Gene upregulation	ASODN (luciferase)	RCA	Ovarian cancer (SKOV3)	38
	saRNA (p21)	RCT	Prostate cancer (PC3)	40
	mRNA (Apoptin)	RCT	Breast cancer (4T1)	42
Immunostimulant	Immunostimulant (CpG ODN)	RCA	Bone marrow-derived dendritic cells	45
Catalysis	Immunostimulant (dsRNA)	RCT	Ovarian cancer (SKOV3)	16
	DNAzyme (EGR-1)	RCA	Breast cancer (MCF-7)	46
Drug loading	DNAzyme (EGR-1)	RCA	Breast cancer (MCF-7)	47
	Chemodrug (mitoxantrone)	RCA	Breast cancer (MCF-7)	53
	Photosensitizer (SiPcCl ₂)	RCT	Cervical cancer (HeLa)	54
Targeting moiety	CRISPR/Cas9 (GFP)	RCT	Cervical cancer (HeLa)	58
	Aptamer (APMAP)	RCA	Obesity (adipocyte)	62
Stimulus dynamics	Aptamer (PD-1, CTLA-4)	RCA	Skin melanoma (B16)	63
	Chemodrug (DOX)	RCA	Cervical cancer (HeLa)	25
	Chemodrug (DOX)	RCA	Cervical cancer (HeLa)	66
	CRISPR/Cas9 (GFP)	RCA	Osteosarcoma (U2OS)	68

Abbreviations: siRNA, small interfering RNA; PLK1, polo-like kinase 1; Bcl2, B-cell lymphoma 2; ASODN, antisense oligonucleotide; saRNA, small activating RNA; mRNA, messenger RNA; CpG ODN, cytosine–guanine oligonucleotide; dsRNA, double stranded RNA; DNAzyme, deoxyribozyme; EGR-1, early growth response protein-1; SiPcCl₂, silicon phthalocyanine dichloride; CRISPR, clustered regularly interspaced short palindromic repeats; Cas9, CRISPR associated protein 9; GFP, green fluorescent protein; APMAP, adipocyte plasma membrane associated protein; PD-1, programmed cell death protein 1; CTLA-4, cytotoxic T-lymphocyte-associated protein 4; DOX, doxorubicin.

delivery. RNA interference (RNAi) is a post-transcriptional gene silencing mechanism regulated by small interfering RNA (siRNA) and microRNA (miRNA), which rapidly modulate gene expression.²⁸ The first polymeric siRNA synthesized using rolling circle transcription (RCT) were reported by Hammond's group.²⁹ Polymeric siRNA, composed of sense and antisense sequences linked by a hairpin loop, self fold into short hairpin RNA (shRNA) like repeats, which are processed by Dicer into siRNA. Serving as both a delivery scaffold and Dicer activated prodrug, these densely packed RNA polymers offer enhanced biostability, efficient siRNA loading, and potent gene silencing efficacy.³⁰ Subsequent investigations have underscored the gene regulatory versatility of polymeric siRNA, demonstrating their capacity to modulate multiple targets by incorporating distinct siRNA sequences,³¹ or improve therapeutic efficacy by structural modulation of RCR based nanostructures^{32–34} compared to that of monomeric form. miRNA exhibits features distinct from those of siRNA, in that it is endogenously expressed, shows partially complementary binding to messenger RNA (mRNA), and broadly modulates gene expression.³⁵ An RCT based miRNA drug delivery system was developed by encoding the miRNA-34a sequence onto polymeric RNA.³⁶ The polymeric miRNA retained their original function as tumor suppressors by regulating silent information regulator 1 (SIRT1) expression, thus inhibiting the proliferation of cancer cells. Antisense oligonucleotide (ASODN) binds complementarily to target mRNA, leading to gene downregulation through RNase H-mediated degradation or by sterically blocking ribosomal translation.³⁷ The first polymeric ASODN produced *via* RCA showed significantly enhanced intrinsic stability and gene downregulation compared to that with conventional monomeric ODNs, showing improved resistance under physiological

conditions.³⁸ Moreover, polymeric ASODN revealed minimal bladder accumulation, suggesting their potential for *in vivo* therapeutic applications. Such nucleic acid based gene downregulation strategies enable the precise silencing of disease-associated genes, minimizing off target effects, and modulation of previously 'undruggable' targets, thereby broadening the therapeutic landscape.

2.2. Gene upregulation

Gene upregulation using nucleic acid based approaches is emerging as a powerful strategy with significance comparable to that of gene downregulation. In contrast to RNAi, small activating RNA (saRNA) promotes transcriptional activation by targeting gene promoters in the nucleus.³⁹ This approach has been used in several studies to upregulate endogenous gene expression for therapeutic purposes. RCT based nanostructures encoding tandem saRNA undergo Dicer mediated processing into monomeric saRNA that are subsequently incorporated into Ago2 containing RNA induced transcriptional activation complexes.⁴⁰ The antisense strand of the saRNA guides the complex to the promoter region of the target gene, thereby facilitating transcriptional activation. This activation promotes apoptosis in cancer cells by upregulating p21 expression, thereby presenting a novel strategy for gene therapy. mRNAs convey genetic information from DNA to ribosomes for protein synthesis.⁴¹ As a therapeutic modality, mRNAs enable transient and controllable expression of functional proteins. Efficient and sustained translation of encoded proteins has also been achieved using RCT based polymeric mRNA nanoparticles.⁴² The encoding of therapeutic proteins in polymeric RNA was demonstrated using RCT on an engineered apoptin plasmid. The RCT based transcript exhibited efficient therapeutic

apoptin expression in cancer cells, which enhanced tumor tissue necrosis and demonstrated effective gene therapy for breast cancer *in vivo*. Thus, promoting the expression of beneficial genes through gene upregulation offers therapeutic potential for diseases characterized by insufficient gene expression.

2.3. Immunostimulation

Nucleic acids are being increasingly recognized for their ability to modulate immune responses *via* pattern recognition receptor activation.⁴³ For example, unmethylated cytosine–guanine oligonucleotide (CpG ODN) and long double stranded RNA (dsRNA) have been extensively explored as immunostimulants for immune related therapeutics, including for cancer and allergy. Once internalized, these sequences bind to pattern recognition receptors (PRRs) such as Toll like receptor 9 (TLR9) and Toll like receptor 3 (TLR3), triggering downstream signaling pathways that lead to the production of proinflammatory cytokines and type I interferons. RCA based polymeric CpG ODN can overcome the therapeutic hurdles associated with conventional CpG ODN by enhancing their immunostimulatory potency and physiological stability, thereby advancing their applicability as immunomodulatory adjuvants in cancer immunotherapy.^{44,45} The use of polymeric CpG ODN as a cancer treatment was demonstrated using catalase cored nanoparticles loaded with polymeric CpG ODN *via* RCA and copper ions. The nanoparticles were delivered in tumor cells and copper ions induced cuproptosis-mediated immunogenic cell death, resulting in dendritic cell maturation. Catalase improved immunosuppressive tumor microenvironment and the polymeric CpG ODN promoted dendritic cell maturation by activating TLR9 to enhance antigen presentation, collectively eliciting a long term antitumor immune response. In parallel, RCT based long double stranded RNA (dsRNA), which resembles viral genetic material, has proven to be a potent activator of the innate immune system, promoting proinflammatory cytokine production and enhancing antigen presentation and immune cell activation.¹⁶ These findings suggest that polymeric dsRNA serves as a dual-function agent in cancer therapy—facilitating gene silencing *via* RNAi and inducing immunostimulation as dsRNA. Overall, nucleic acid based immunostimulants can be loaded into programmable and biocompatible nucleic acid nanostructures for modulating immune responses in therapeutic applications.

2.4. Catalysis

Certain nucleic acid structures possess intrinsic catalytic activity that can induce sequence-specific cleavage of target nucleic acids. Deoxyribozymes (DNAzymes) are ssDNA molecules that have emerged as promising therapeutic agents owing to their ability to selectively cleave target RNA or DNA sequences within cells. This cleavage downregulates the expression of disease-associated proteins, thereby exerting therapeutic effects. Despite their therapeutic potential, DNAzyme based therapies face key challenges, including poor cellular uptake and limited intracellular availability of essential metal ion cofactors. In this context, RCA based polymeric DNAzymes can downregulate the expression of target proteins and facilitate DNAzyme based

gene therapy.⁴⁶ For instance, two types of DNAzymes have been designed for sequential cascade enzymatic reactions in which metal ions function as cofactors. In particular, the negative charge of polymeric DNAzymes within nanocarriers enables electrostatic interactions with the positive charge of metal cofactors, thereby facilitating localized supplementation of the essential metal ions required for optimal catalytic activity.⁴⁷ Ribozymes are RNA molecules with catalytic activity that can specifically cleave target RNA sequences through catalytic reactions without the need for protein cofactors.⁴⁸ Owing to these properties, RCT based self-cleaving concatemeric ribozymes offer a promising approach for the automatic production of therapeutic RNAs. Polymeric ribozymes are subsequently assembled either *in situ* or *via* one pot co-transcription to construct RNA nanostructures with defined motifs and functionalities. This technique facilitates large scale therapeutic RNA manufacturing strategies that streamline the production process.⁴⁹ These cleavage based systems enable direct post-transcriptional gene silencing without relying on the RNAi pathway, thereby offering an alternative gene therapy strategy. Furthermore, the self-cleaving motifs facilitate controlled degradation, thereby supporting the design of responsive transient therapeutic systems.

2.5. Drug loading

Nucleic acids serve as versatile scaffolds for cargo delivery because of their programmable architecture and predictable base pairing. Diverse small molecules, such as those for anti-cancer therapeutics, can be loaded into the nucleic acid scaffolds *via* π – π stacking interaction between planar aromatic structures of the small molecules and the nucleobases, as well as intercalation into the nucleic acid duplex.^{50,51} These interactions are widely used in drug delivery systems by intercalating chemotherapeutic drugs,^{52,53} photosensitizers,⁵⁴ and photothermal agents.⁵⁵ RCR based nucleic acid nanostructures allow ultra-long nucleic acid sequences for enhanced drug loading and efficient delivery to cancer cells. In addition, RCR based nucleic acid nanostructures can be rationally designed to include specific complementary binding regions, enabling the hybridization of oligonucleotides. This strategy allows for the programmable loading of therapeutic agents *via* sequence-specific base pairing, offering a modular and versatile platform for nucleic acid based drug delivery systems. For example, nucleic acid nanostructures, the RNA triple helix, self assemble two distinct therapeutic miRNAs into a highly stable RNA configuration, thereby enhancing the co-transfection efficiency in cancer cells.⁵⁶ Taking advantage of the RNA triple helix structure, an RCT based RNA triple helix hydrogel was developed for treating triple negative breast cancer. Polymeric RNA scaffolds were engineered to complementarily hybridize two therapeutic miRNAs, miRNA-205 and anti-miRNA-221, resulting in hydrogel formation. This design enabled the efficient co-delivery of dual miRNA therapeutics without the need for synthetic polycationic carriers, ultimately achieving synergistic inhibition of tumor progression.⁵⁷ The clustered regularly interspaced short palindromic repeats (CRISPR) and CRISPR-associated protein 9 (CRISPR/Cas9) system enables precise genome editing by inducing double strand breaks

at target DNA sites guided by a single guide RNA (sgRNA), offering the potential for gene targeted drug delivery. RCT based polymeric RNA can also serve as a scaffold for loading Cas9 protein by directly incorporating the sgRNA sequence, thereby facilitating formation of the CRISPR Cas9 complex.⁵⁸ Co-delivery of chemodrug and siRNA was achieved by the intercalation of doxorubicin (DOX) and complementary hybridization of siRNA onto RCA based polymeric DNA. The addition of oligonucleotides, designed to partially hybridize with both polymeric DNA and siRNA, resulted in RCA based nanoassemblies.⁵⁹ In the cytosolic environment, hybridized siRNA was released by enzymolysis, which subsequently downregulated signal transducer and activator of transcription 3 (STAT3), resulting in a synergistic anticancer effect with DOX in cancer cells. These delivery platforms based on polymeric nucleic acids allow for enhanced loading capacity and precise control over spatial distribution, positioning them as state-of-the-art drug delivery systems.

2.6. Targeting moiety

By specifically recognizing cell surface receptors or disease-associated biomarkers, targeting specific moieties can enhance therapeutic efficacy while minimizing off target effects in drug delivery systems. Aptamers are short single-stranded nucleic acids that can fold into distinct three-dimensional structures, enabling them to bind specifically and with high affinity to a wide range of target molecules.⁶⁰ Numerous studies have employed RCR based polymeric aptamers by incorporating aptamer sequences into template DNA. The resulting ultra-long tandem repeats show significantly enhanced targeting capability, biostability, and mechanical properties, making them particularly advantageous for applications in targeted therapy.⁶¹ The adipo-8 aptamer, targeting adipocyte plasma membrane-associated protein on mature adipocyte membranes, reduces body weight and blood triglyceride levels. RCA based nanoparticles incorporating tandem adipo-8 aptamer sequences on polymeric DNA have thus been developed for targeted delivery to mature adipocytes, suggesting the potential applicability of adipo-8 as a therapeutic agent for obesity.⁶² In cancer immunotherapy, aptamers function as immune checkpoint inhibitors by binding to immune checkpoint receptors. Accordingly, an RCA based hydrogel was engineered using two polymeric DNA aptamers targeting programmed cell death protein 1 and cytotoxic T-lymphocyte-associated protein 4.⁶³ Aptamers are released from DNA hydrogels in response to an inflammatory microenvironment, thereby exerting therapeutic effects as immune checkpoint blockades. Further, polymeric aptamer considerably enhanced their *in vivo* binding affinity compared to monomeric aptamer, as polymeric form can improve biological function and biostability in physiological environments with escape from renal clearance.⁶⁴

2.7. Stimulus dynamics

Nucleic acids can be rationally designed to undergo conformational changes or structural disassembly in response to specific stimuli. The i-motif is a pH sensitive, noncanonical DNA secondary structure formed by cytosine rich sequences, particularly under mildly acidic conditions.⁶⁵ It is stabilized through

the formation of intercalated hemi protonated cytosine–cytosine (C–C⁺) base pairs, resulting in a compact quadruplex conformation. This structural motif exhibits reversible conformational transitions in response to changes in environmental pH. Owing to its pH responsiveness and structural tunability, the i-motif has garnered significant interest as a functional moiety for designing stimuli responsive nucleic acid based drug delivery platforms. In this context, i-motif sequences can be encoded in the RCA template, resulting in the generation of ultra-long polymeric DNA strands containing tandemly repeated i-motif domains. RCA based polymeric i-motif structures can serve as pH responsive drug delivery platforms, wherein the acidic tumor microenvironment (TME) induces conformational changes in the i-motif domains.⁶⁶ Chemotherapeutic drugs intercalated within RCA based polymeric i-motif sequences can then be effectively released under acidic conditions. The presence of pH responsive i-motif structures enables conformational changes in the TME, facilitating drug release, and enhancing anticancer efficacy. Another notable application of i-motif structures is in hydrogel platforms. RCA based polymeric DNA hydrogels incorporating aptamers and i-motif sequences successfully facilitated the release of intercalated DOX upon exposure to the acidic TME.²⁵ The hydrogel was injected intratumorally, demonstrating its potential as a stimuli responsive platform for localized cancer therapy. Toehold-mediated strand displacement is a sequence-specific mechanism in which an incoming strand binds to an exposed single-stranded toehold, initiating branch migration and displacing a prebound strand.⁶⁷ This process enables precise control over dynamic nucleic acid systems such as programmable drug release.⁶⁸ RCA based polymeric DNA scaffolds can function as miRNA responsive carriers for the cytosolic delivery of Cas9/sgRNA complexes into tumor cells. The scaffold is designed with a hybridization site complementary to both miRNA-21 and sgRNA. This design allowed endogenous miRNA-21 to displace the initially bound Cas9/sgRNA complex *via* toehold-mediated strand displacement, thereby enabling the release of the complex to exert gene regulation.⁶⁹ This stimulus responsiveness enables spatiotemporal control over drug release, thereby improving the therapeutic index while minimizing systemic toxicity.

3. Engineering strategies

RCR based concatemeric strands tend to self organize into densely entangled or condensed architectures referred to as microsponges. Structurally, these microsponges are classified as organic–inorganic particles comprising supramolecular DNA or RNA entangled with magnesium pyrophosphate (MgPPi) crystals (Fig. 2A).⁷⁰ During RCR, DNA or RNA polymerases, such as Phi29, Taq, T7, T3, or SP6, catalyze nucleic acid synthesis, thus yielding pyrophosphate (PPi) as a byproduct (Fig. 2B). The PPi rapidly chelates magnesium ions in the buffer to form MgPPi crystal sheets, which act as nucleation centers. These growing inorganic domains interact electrostatically with

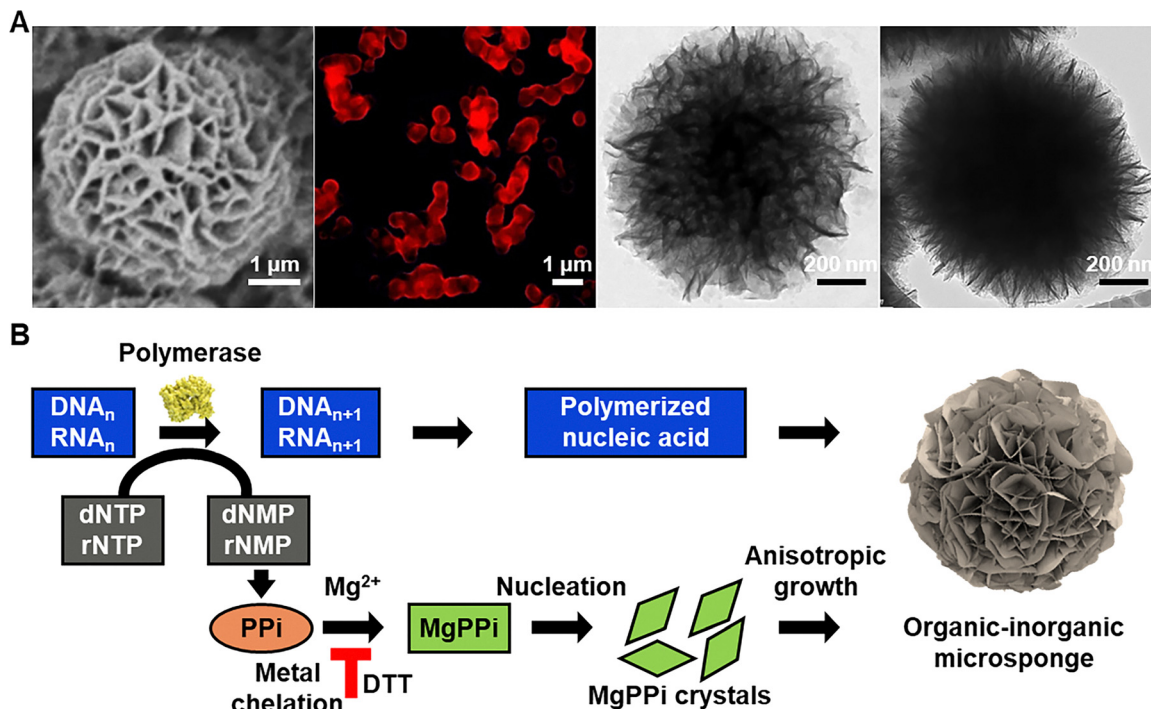


Fig. 2 Synthesis of organic–inorganic hybrid nucleic acid particles *via* rolling circle replication (RCR). (A) Morphology and structure analyses of organic–inorganic hybrid nucleic acid particles with scanning electron microscopy, confocal laser scanning microscopy, transmission electron microscopy, and cryo-transmission electron microscopy. Reproduced with permission from ref. 31 Copyright 2021, American Chemical Society. (B) Scheme for mechanism of the organic–inorganic hybrid nucleic acid particles formation during RCR. Reproduced with permission from ref. 25 Copyright 2023, Elsevier Ltd. dNTP, deoxyribonucleotide triphosphate; dNMP, deoxyribonucleotide monophosphate; rNTP, ribonucleotide triphosphate; rNMP, ribonucleotide monophosphate; Mg²⁺, magnesium ions; DTT, dithiothreitol.

the polymeric nucleic acids to form hybrid microsponge networks. Considering the reaction dependency of microsponge formation, fine tuning the enzymatic kinetics and ionic composition provides a means to control properties such as nucleic acid length, size, crystallinity, polymorphism, surface charge, and structural stability of the microsponge. In this section, we aim to consolidate these strategies into a coherent framework to better understand the rational engineering of microsponge formation and their functions for programmable drug delivery.

3.1. Size controlled synthesis

Given the critical importance of particle size in drug delivery applications, extensive efforts have been made to control the size of microsponges synthesized using RCR. Among various influencing factors, parameters such as reaction duration, concentration of the circular DNA template, nucleotide-to-polymerase ratio, and chemical modifications of nucleotides have been shown to play pivotal roles in generating size-controllable and monodispersed nucleic acid particles.

One of the most straightforward and direct parameters for regulating particle size is the duration of the amplification reaction. As RCR proceeds, DNA or RNA polymerase continuously extend the nascent strand by displacing the previously synthesized product, resulting in the elongation of ssDNA or single stranded RNA coils. This ongoing elongation directly contributes to increased nucleic acid length, structural

complexity, and larger final particle size.^{71,72} Moreover, the concentration of the circular DNA template affects the overall yield and growth of the microsponge architecture.^{73,74} An increase in template concentration or a higher ribonucleotide triphosphate-to-polymerase ratio tends to enhance the replication throughput, leading to larger and more entangled structures (Fig. 3A).^{18,19} These structures maintain the size differences after post-modification with functional polymers to enhance therapeutic efficacy. More importantly, the size-mediated surface-to-volume ratio plays a critical role in systematic delivery, intracellular delivery, and gene regulation efficiency. A consistent trend across studies suggests that particle size is closely correlated with replication kinetics; that is, particles tend to grow larger when the replication process proceeds rapidly and without interference.

To expand the functional versatility of microsponges, chemically modified deoxyribonucleotide triphosphates, such as azidomethyl-, ethynyl-, and aminopropynyl-substituted nucleotides, have been incorporated into the RCR process. Although these modifications offer potential for post-synthetic functionalization and bioconjugation, their incorporation often results in reduced replication efficiency. Consequently, a higher concentration of such modified nucleotides leads to smaller microsponge sizes owing to hindered strand elongation.⁷⁵ Ultimately, tuning the size of RCR based particles offers a strategic advantage in regulating their surface-to-volume ratio,

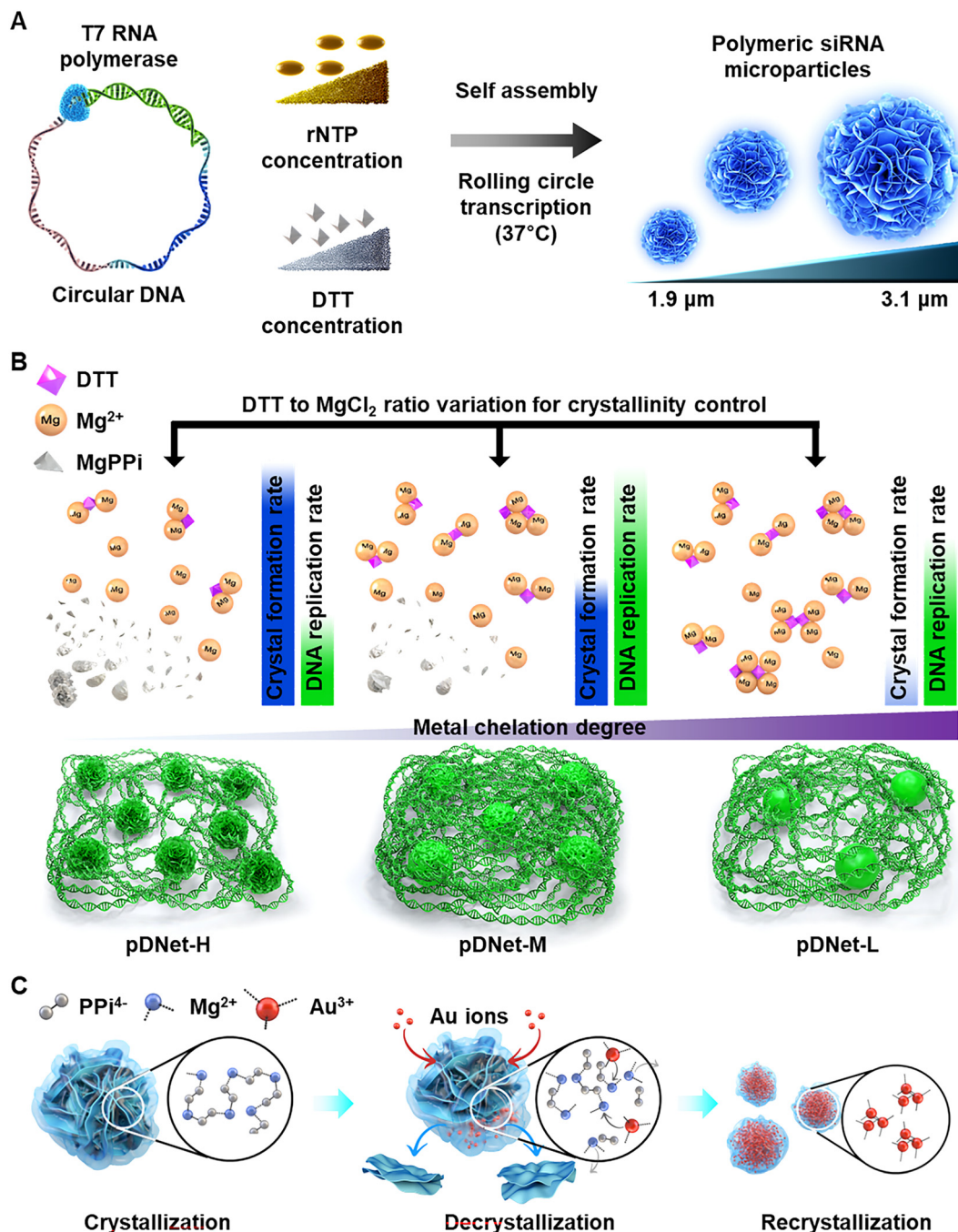


Fig. 3 Physicochemical property-tuned rolling circle replication (RCR) based nucleic acid nanostructures engineering strategies. (A) Size-controlled organic–inorganic nucleic acid nanostructures with different concentrations of rNTP and DTT. Reproduced with permission from ref. 18 Copyright 2024, American Chemical Society. (B) Crystallinity-controlled organic–inorganic nucleic acid nanostructures with different DTT ratios. Reproduced with permission from ref. 25 Copyright 2023, Elsevier Ltd. (C) Morphology-controlled organic–inorganic nucleic acid nanostructures via metal ion-induced reconfiguration. Reproduced with permission from ref. 24 Copyright 2024, Wiley-VCH GmbH, Weinheim. rNTP, ribonucleotide triphosphate; DTT, dithiothreitol; siRNA, small interfering RNA; Mg^{2+} , magnesium ions; MgPPI, magnesium pyrophosphate; $MgCl_2$, magnesium chloride; pDNet-H, polymeric DNA network-high crystallinity; pDNet-M, polymeric DNA network-medium crystallinity; pDNet-L, polymeric DNA network-low crystallinity; PPi^{4-} , pyrophosphate ions; Au^{3+} , gold ions.

which significantly affects their interactions with biological targets such as cells, receptors, and proteins. This ability to fine tune the particle size has profound implications for enhancing the performance of nucleic acid nanostructures in specific drug delivery applications.

The size of RCR-derived microsponges is governed by a delicate interplay between replication kinetics and compositional parameters. Thus, modulating reaction time, template concentration, nucleotide chemistry, and enzyme-to-substrate ratios provides a versatile toolbox for tailoring particle dimensions

to specific biomedical needs. Given the strong correlation between particle size, surface-to-volume ratio, and biological performance, precise control over these parameters not only enables the optimization of delivery efficiency but also expands the functional scope of nucleic acid based nanostructures.

3.2. Crystallinity controlled synthesis

Just as the kinetics of nucleic acid replication strongly influence particle size, they also govern the nucleation and crystal growth dynamics of the resulting organic-inorganic composite structures. Recent studies have demonstrated that the deliberate tuning of biochemical reaction components can manipulate the morphology, crystallinity, and complexity of RCR based microsponges. Among these, a particularly insightful approach involves modulating the balance between the metal chelating agent dithiothreitol (DTT) and polymerase concentration (Fig. 3B).²⁵ DTT is commonly employed as both a polymerase stabilizer and reducing agent that enhances the overall reaction efficiency. However, when present in excess, DTT competes with essential divalent cations, particularly magnesium ions (Mg^{2+}), for binding in the reaction buffer. Magnesium plays a central role in nucleic acid replication and crystallization. Excess DTT reduces the availability of free Mg^{2+} for nucleotidyl transfer and PPi precipitation, thereby slowing replication kinetics and yielding poorly crystalline, transparent, and polymeric DNA networks instead of well-defined microsponges.⁷⁶

In addition to redox control, direct adjustment of divalent ion concentrations, especially that of magnesium, has been shown to affect particle complexity, size, and degree of crystallinity.⁷⁷ Magnesium ions are integral to both the enzymatic catalysis and structural formation of RCR particles. Specifically, Mg^{2+} plays multiple roles during polymerase-mediated replication, acting as an activator of nucleophilic attack in phosphodiester bond formation and functioning as an electrostatic shield for the negatively charged phosphate backbone of nucleic acids.⁷¹ During RCR, Mg^{2+} coordinates with phosphate groups, acidic polymerase residues, and water molecules, facilitating the release of PPi. Free Mg^{2+} in solution readily binds with PPi^{4-} to form Mg_2PPi , which subsequently precipitates. The resulting interaction between Mg_2PPi and nucleic acids leads to the formation of hybrid nanostructures, in which long, flexible RNA (or DNA) strands act as scaffolds to mediate the nucleation and crystal growth of Mg_2PPi .^{30,70}

These compositional changes in the inorganic framework of nucleic acid networks have been shown to affect surface area modulation, a key factor in enhancing the functionality of the final material. For instance, optimizing these hybrid compositions enables more efficient interactions with target biomolecules such as aptamer sequences, thereby improving their performance in advanced drug delivery.

3.3. Morphology variations

RCR based nucleic acid composite structures are primarily composed of replicated nucleic acid strands intertwined with Mg_2PPi crystals. The distinctive flower-like morphology of these microsponges is attributed to the crystallographic nature

of Mg_2PPi . However, recent studies have explored the use of alternative divalent ions, such as cobalt (Co^{2+}) and manganese (Mn^{2+}), instead of magnesium during the RCR process to modulate the morphology and extend the functional applicability of the resulting structures. In addition, the post-modification of microsponges with biofunctional polymers or metal ions can disrupt the crystalline structure, reduce the particle size, and modulate the surface size to be more appropriate for programmable drug delivery. Significant variations in particle morphology, size, and DNA content have been reported depending on the metal ion species, metal concentration, and type of polymerase employed.^{21,22} For example, microsponges synthesized using Mn^{2+} ions exhibit a layered, hasselback-like structure, whereas Co^{2+} based structures exhibit sharp, spiky petals that form a more aggressive flower-like geometry. This strategic ion substitution opens new pathways for engineering RCR based microstructures as functional nucleic acid carriers, cell tracking agents, and for magnetic resonance imaging, broadening their utility in advanced drug delivery applications.

Beyond ionic substitution, microsponge properties can be finely tuned for biomedical applications through structural condensation strategies such as electrostatic condensation, a widely adopted technique. Owing to the inherent anionic nucleic acids on their phosphate backbones, the introduction of cationic polymers promotes strong electrostatic interactions, leading to the collapse of the original flower-like crystalline structure,^{31,37} resulting in the formation of polyplex structures composed of nucleic acids condensed with cationic polymers. This condensation dramatically reduces the particle size by approximately ten-fold and imparts a positive surface charge, thereby enhancing intracellular delivery efficiency. Following condensation, a layer-by-layer assembly of negatively charged functional polymers has been employed to further optimize the particles as nanocarriers, allowing programmable drug loading, disease targeting, and drug release profiles.

Additionally, innovative hybridization approaches have recently emerged in which gold (Au^{+}) or silver (Ag^{+}) ions are bound to DNA microsponges through aptamer-metal interactions.^{23,78} Subsequent chemical reduction with DTT or $NaBH_4$ yields metal nanoclusters embedded in the polymeric DNA nanostructure matrix. During this process, the original flower-like microsponge morphology collapses, and the resulting structure is a dense, homogeneous nanoparticle composed of DNA and metallic clusters. In Au hybridized microsponges, the use of DNA microsponges as reduction templates ensures a high density and uniform distribution of metal nanoclusters (Fig. 3C).²⁴ Notably, these hybrid microstructures retain the intrinsic properties of metal nanoclusters, such as their near-infrared (NIR) responsiveness, fluorescence, and antibacterial activity, making them highly attractive for multifunctional drug delivery systems.

Taken together, these hybridization and condensation approaches provide a robust toolbox for diversifying the structural and functional landscapes of RCR based microsponges, thereby significantly expanding their utility in interdisciplinary nanotechnology for drug delivery.

3.4. Circular DNA template variations

Building on strategies involving physicochemical modulation and hybrid material formation, another dimension of control arises from the inherent programmability of nucleic acid sequences. This molecular level design facilitates precise manipulation of network density, mechanical stability, and biological functionality, addressing fundamental challenges such as the low intrinsic stability of nucleic acid materials.

One representative approach involves the use of multiple primers that bind to the replicated ssDNA sequences during RCA.⁷⁹ These primers act as additional initiation sites for polymerase attachment and extension, thereby increasing the number of replication fronts and producing a denser DNA network. This method, known as multi-primed chain amplification (MCA), enables control over the entanglement density of DNA microsponges. By modulating the reaction durations of RCA and MCA, researchers have demonstrated a direct correlation between primer availability, network tightness, and structural integrity, thus achieving improved stability compared with that of conventional RCA based constructs. Another strategy leverages sequence complementarity by employing multiple circular DNA templates designed to yield replicated nucleic acids that hybridize with one another.²⁷ This approach has been particularly effective for RNA based systems, which traditionally suffer from poor stability and limited network formation capabilities. Through complementary sequence design, polymeric RNA strands can self-assemble into stable networks, resulting in RNA membranes with significantly enhanced biostability. These improvements are achieved without additional chemical modifications, relying solely on the rational adjustment of template sequences, thereby offering a minimal yet powerful strategy for stabilizing functional RNA materials for drug delivery.

In addition to structural enhancement, sequence programmability enables the creation of selective recognition systems using base pair hybridization logic.⁸⁰ In one such approach, a circular DNA template is designed to encode a target binding domain such as an aptamer sequence, which is replicated using RCA to form the first layer DNA network. Upon incubation with a specific biological target, the second DNA network, generated through RCA with a complementary sequence, is introduced. Hybridization between the two networks enhances stability and causes massive complexation, leading to sedimentation of the target–network complex. This phenomenon has been utilized for selectively sequestering and isolating rare stem cells from mixed populations, relying on the precise selectivity of DNA hybridization. The captured cells can be enzymatically released by DNase treatment, illustrating the reversible and programmable nature of this nucleic acid based targeting strategy.

These sequence driven design strategies complement and enhance the physical and chemical control methods discussed previously, collectively enabling a comprehensive framework for engineering RCR based nucleic acid nanostructures with tunable morphologies, enhanced biostability, and application-specific molecular functions including drug delivery.

4. Programmable drug delivery

Advances in RCR based nucleic acid nanostructures have significantly enhanced the development of targeted drug delivery systems. These innovations leverage the unique properties of nucleic acid nanostructures, such as programmability, biocompatibility, and precise functionalization, to improve their therapeutic efficacy and minimize undesired side effects. In this section, we discuss a key feature of RCR based nanostructures for their programmable design, which enables versatile delivery strategies. These include passive targeted delivery, which relies on physiological phenomena such as the enhanced permeability and retention (EPR) effect and lymphatic drainage; active targeted delivery, which involves ligand–receptor interactions or tuning of nanoparticle size and surface characteristics; and stimuli responsive delivery, which is engineered to specifically release therapeutic agents to disease sites in response to internal or external triggers such as pH, redox gradients, or light.

4.1. Passive targeted delivery

RCR based nucleic acid nanostructures have contributed significantly to passive drug delivery by enabling the scalable synthesis of dense, programmable carriers with tunable size, surface charge, and high payload capacity. These properties are particularly beneficial for promoting EPR-mediated tumor accumulation and lymphatic drainage based targeting in immunotherapy.

Given that nanoparticles migrate to lymph nodes *via* lymphatic drainage after injection, Zhu *et al.* developed intertwining DNA–RNA nanocapsules (iDR-NCs) as a multifunctional nanovaccine for cancer immunotherapy, enabling the co-delivery of CpG ODN, shRNA, and tumor-specific peptide neoantigens.⁴³ Tandem CpG ODN and shRNA strands were generated *via* simultaneous RCA and RCT, forming microflowers that were condensed into nanoscale capsules using a polyethylene glycol (PEG)-grafted cationic polypeptide, followed by the loading of neoantigens into the nanocapsules. *In vivo* studies have shown that iDR-NCs effectively target antigen-presenting cells (APC) in lymph nodes *via* lymphatic drainage following subcutaneous administration. Co-delivered CpG ODN and shRNA synergistically activate APC, promoting CD8⁺ T cell responses and tumor suppression, revealing the potential of RCA/RCT based nanostructures for passive targeting *via* lymphatic transport.

Complementary RCT (cRCT) using two types of circular DNA with complementary sequences has been attempted to synthesize more densely packed polymeric RNA nanostructures. To avoid nonfunctional short dsRNA and increase efficient siRNA release by Dicer cleavage of cRCT, Kim *et al.* synthesized bubbled RNA based cargos (BRCs) comprising polymeric siRNA with a bubble region.⁸¹ The densely packed siRNA suppressed UBA6 specific E2 conjugating enzyme 1 (USE1) expression, inducing cell cycle arrest and apoptosis, thereby inhibiting proliferation and invasiveness in A549 and HeLa cancer cells. In addition, repeated intravenous administration of BRCs

induced efficient accumulation at the tumor site and tumor growth suppression in A549 xenograft mouse model. These findings establish USE1-targeted BRCs as a potent RNAi platform with promising clinical potential for cancer therapy.

Among the strategies to enhance the intracellular delivery efficiency in passive targeted delivery, control of nanoparticle shape has been attempted. Kim *et al.* synthesized cationic

cellulose nanocrystals (CNCs) complexed with polymeric siRNA, synthesized *via* RCT, using a material based approach (Fig. 4A).⁸² CNCs were obtained *via* acid hydrolysis of plant-derived cellulose and functionalized with cationic groups to enable electrostatic complexation. Notably, their rod-shaped morphology (100–300 nm in length and high aspect ratio) facilitated faster cellular internalization and enhanced tumor accumulation *via* the EPR

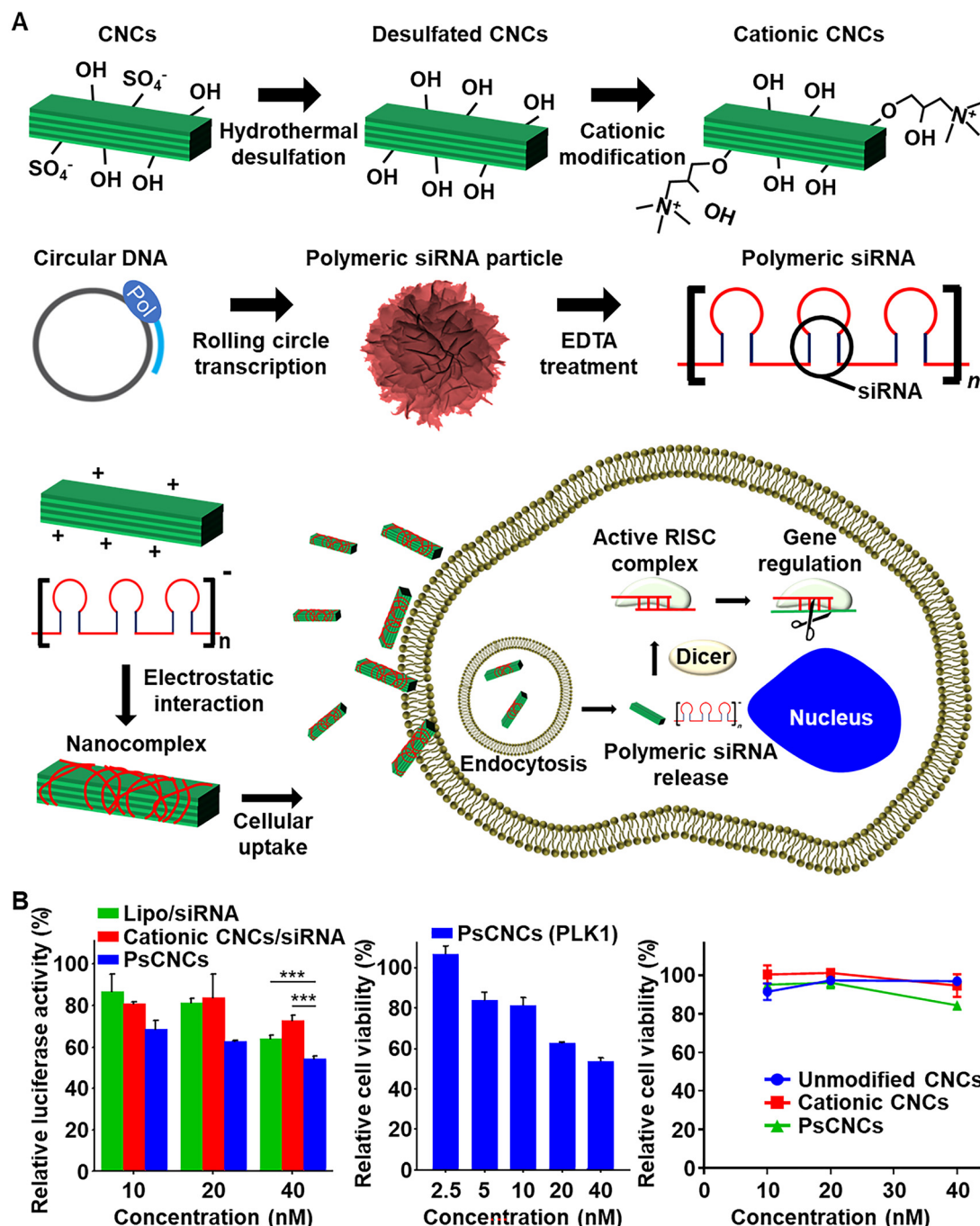


Fig. 4 Polymeric siRNA/cationic cellulose nanocrystals (CNCs) nanocomplex (PsCNCs) for efficient anticancer drug delivery. (A) Scheme for synthesis of cationic CNCs, polymeric siRNA, and PsCNCs. (B) Gene silencing efficacy, anticancer effect, and biocompatibility in SKOV3 cells of PsCNCs. Reproduced with permission from ref. 82 Copyright 2020, Elsevier Ltd. siRNA, small interfering RNA; EDTA, ethylenediaminetetraacetic acid; Lipo, lipofectamine; PLK1, polo-like kinase 1.

effect compared to that of spherical nanoparticles. Strong electrostatic interactions between cationic CNCs and anionic polymeric siRNA provided effective protection against RNase A degradation. Furthermore, by leveraging their rod like shape, the nanoparticles significantly improved the intracellular delivery and gene silencing efficiency of the polymeric siRNA (Fig. 4B).

To enhance antitumor immunity, RNA nanoadjuvant for APC and tumor cells have been developed. Xu *et al.* demonstrated a self-assembled RNA nanoadjuvant synthesized by RCT and further modified with cationic liposomes to enhance APC-mediated antitumor immunity.⁸³ The densely packed long RNA scaffold activates RIG-I/MDA5 signaling within APC, promoting dendritic cell maturation and polarizes tumor associated macrophages toward an M1 like phenotype. Moreover, the RCT template encodes dual siRNAs targeting CD47 on tumor cells and SIRP α on APC, thereby effectively inhibiting the CD47-SIRP α checkpoint. This combined strategy of innate immune activation and checkpoint blockade enhances APC phagocytic activity, cross-priming of effector T cells, and overall antitumor immune responses, offering a versatile RNA based nanoadjuvant platform for cancer immunotherapy.

Taking advantage of the fact that the RCT reaction produces nanoparticles of various sizes, isolation of those smaller than 100 nm for effective passive targeted delivery were reported. Han *et al.* synthesized sub-100 nm polymeric RNA nanoparticles (RNPs), encoding a TNF- α siRNA sequence *via* RCT.⁸⁴ The RNPs were modified with PEG to enhance systemic delivery for traumatic brain injury (TBI). These polymeric RNPs demonstrated potent *in vitro* knockdown activity and were efficiently internalized by murine microglial cells. PEGylation conferred an extended circulatory half-life and enabled passive targeting, leading to significantly greater accumulation in injured brain tissue in a mouse TBI model. Systemic administration of the PEGylated nanoparticles resulted in RNAi-mediated suppression of TNF- α in the injured brain.

Overall, these studies illustrated how RCR based nanostructures can be programmed to serve as highly versatile scaffolds for passive targeted delivery. By exploiting intrinsic structural features, such as porosity, particle geometry, and size tunability, researchers have developed nanocarriers that accumulate efficiently in tumors *via* the EPR effect and promote lymphatic drainage without the need for active targeting ligands. Their biocompatibility, modularity, and ability to accommodate large nucleic acid payloads further underscores their potential in cancer therapy. Continued efforts to refine shape control, biodegradability, and *in vivo* pharmacokinetics will be key to translating these structurally optimized platforms into preclinically viable therapeutics.

4.2. Active targeted delivery

Recent progress in RCR based nucleic acid nanostructures has enabled the development of precise and effective systems for actively targeted drug delivery. By leveraging the programmability of nucleic acid sequences and modular surface modifications, nanoparticles with high blood circulation times that can

also deliver therapeutic payloads with enhanced cellular specificity and efficiency have been engineered.

While many active targeting systems rely on ligand–receptor interactions, some delivery platforms achieve specificity through cellular uptake pathways and intracellular activation. One such example is a proton activatable DNA nanocarrier (H-DNC) built from RCA generated ultra-long ssDNA for co-delivery of CRISPR/Cas9 ribonucleoprotein (RNP) and DNAzymes.⁴⁸ Compacted with Mn²⁺ and coated with acid degradable polymers, these particles enter cancer cells *via* clathrin- and macropinocytosis-mediated endocytosis. In lysosomes, their coating is degraded by the acidic environment, activating surface-bound HhaI enzymes that cleave the DNA scaffold and release the therapeutic cargo. Cas9 disrupts polo-like kinase 1 (PLK1) expression, while DNAzymes target early growth response protein-1, leading to apoptosis and tumor suppression. This ligand-free system offers a distinct intracellular targeting strategy for cancer gene therapy.

One innovative approach involved the construction of DNA metal nanohybrids by combining RCA-derived ultra-long DNA with gold ions (Au³⁺) to create multifunctional particles for cancer targeting.²⁴ The initial reconfiguration of the RCA-originated hybrid DNA with MgPPi crystals (rohDNA-MgPPi) was performed *via* RCA, to form flower-like structures composed of polymeric DNA and MgPPi crystalline cores (Fig. 5A). Electrostatic interactions with Au³⁺ and DTT reduction reconfigured the structures into condensed RCA-originated hybrid DNA with Au nanostructures with tunable morphology, while preserving functional DNA for AS1411 aptamer (nucleolin targeting) based cancer targeting (Fig. 5B). These nanohybrids exhibited cancer cell-specific targeting *via* nucleolin targeting with low cytotoxicity, and improved NIR absorbance when chemically reduced, suggesting their utility in combined photothermal and gene therapies (Fig. 5C).

A prominent example is the development of dual targeting polymeric siRNA nanoparticles (Dual-PSNPs) for ovarian cancer therapy, which are fabricated *via* RCT-derived siRNA microparticles co-assembled with Mg₂PPi crystals and condensed with PLL to form ~80 nm nanoparticles.³² The system was engineered for dual ligand targeting using HA for CD44 and anti-human epidermal growth factor receptor 2 (HER2) antibodies for the HER2 receptors to achieve receptor-mediated uptake in SKOV3 ovarian cancer cells. Cellular uptake was 2.4-fold higher compared to that of single ligand systems, and PLK1-targeted siRNA delivered *via* Dual-PSNPs achieved ~70% gene knockdown and 34% cancer cell viability at 40 nM siRNA, demonstrating synergistic targeting and cytotoxicity.

To overcome the challenges posed by cellular heterogeneity in hematological malignancies, Kwak *et al.* developed triple-ligand polymeric siRNA nanoparticles (Tri-PSNs) using RCT.³³ These nanoparticles were constructed by condensing polymeric siRNA with PLL and were then functionalized with a combination of three targeting ligands, HA, anti-CD20 antibody, and anti-CD37 antibody, to enable multi-receptor recognition in non-Hodgkin's lymphoma (NHL) cells. Tri-PSNs demonstrated up to a 10-fold increase in intracellular uptake and BCL2 (B-cell lymphoma 2) downregulation in NHL cell lines such as Daudi,

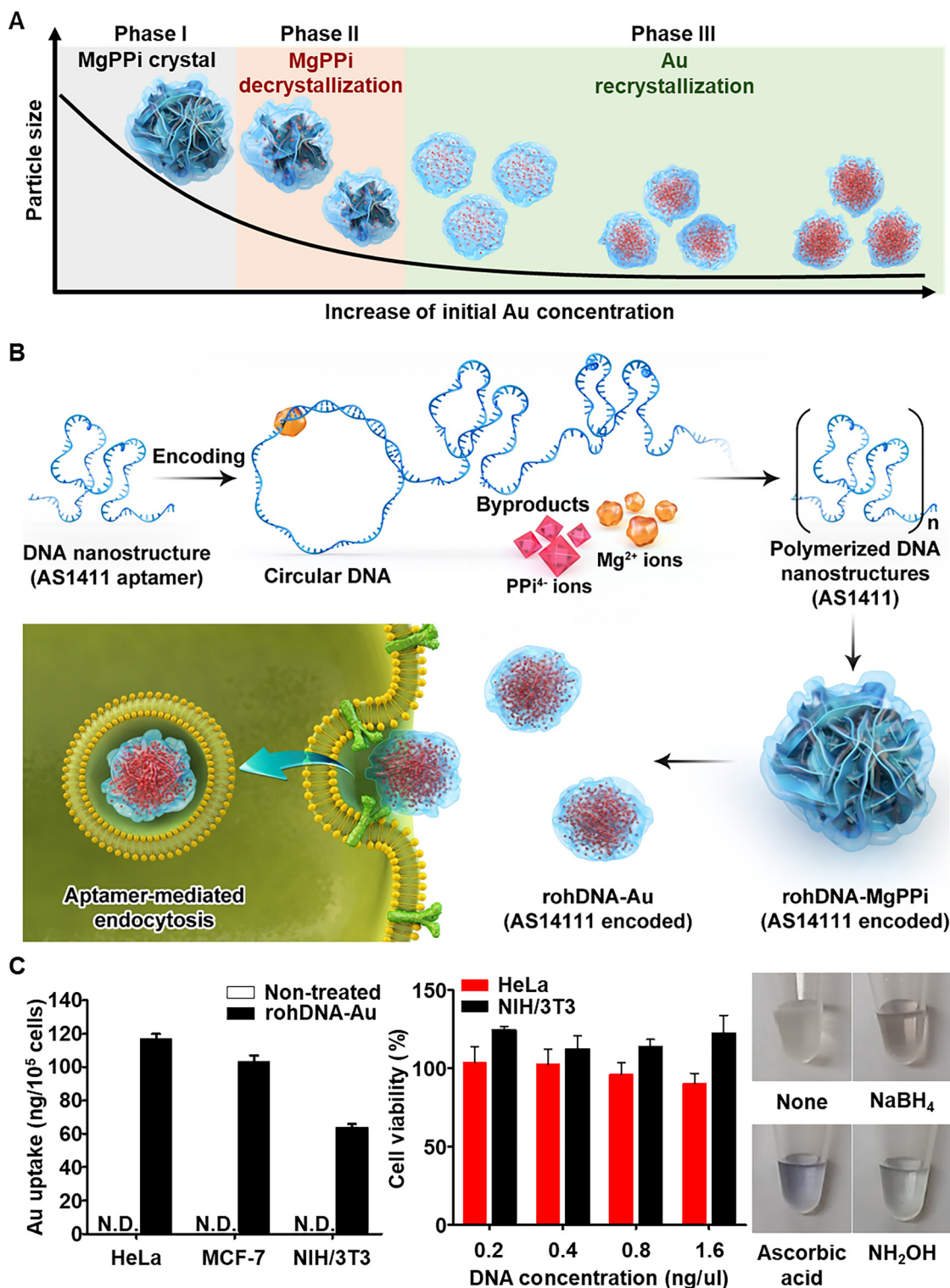


Fig. 5 RCA-originated hybrid DNA with MgPPi crystals (rohDNA-MgPPi) and RCA-originated hybrid DNA with Au nanostructures (rohDNA-Au) for cancer cell targeted delivery. (A) Schematic for crystallization, decrystallization, and recrystallization of rohDNA-MgPPi. (B) Schematic for cancer cell targeted delivery of rohDNA-Au. (C) Intracellular delivery efficiency, biocompatibility, and redox reaction of rohDNA-Au. Reproduced with permission from ref. 24 Copyright 2024, Wiley-VCH GmbH, Weinheim. MgPPi, magnesium pyrophosphate; Au, gold; Mg²⁺, magnesium ions; PPI⁴⁻, pyrophosphate ions; N.D., non detection; NaBH₄, sodium borohydride; NH₂OH, hydroxyl amine.

Raji, and Toledo, compared to that of previously reported monomeric siRNA nanoparticle. At 100 nM siRNA, Toledo cell proliferation was inhibited by 67.5% with negligible cytotoxicity in non-targeted cells. This multi-ligand strategy highlights how the functional programmability of polymeric nanocarriers can effectively address tumor heterogeneity, offering a promising approach for targeted RNA delivery in difficult-to-treat hematological cancers.

Building on ligand-targeting strategies, Kim *et al.* developed polymeric RNA nanoparticles (PRNs) *via* RCT by adjusting the

reaction conditions to generate small-, medium-, and large-sized PRNs (Fig. 6A).¹⁸ These size differences were preserved after condensation with PLL and subsequent layering with either poly-L-glutamate (PLG) or hyaluronic acid (HA) to refine the surface chemistry. The hydrodynamic sizes of the PRNs ranged from 50 to 200 nm with different surface charges, which markedly influenced their *in vivo* biodistribution (Fig. 6B). Among these formulations, the large HA-PRNs (HA-PRN-L, ~150 nm) exhibited superior tumor targeting by combining passive accumulation *via* the EPR effect with CD44-mediated

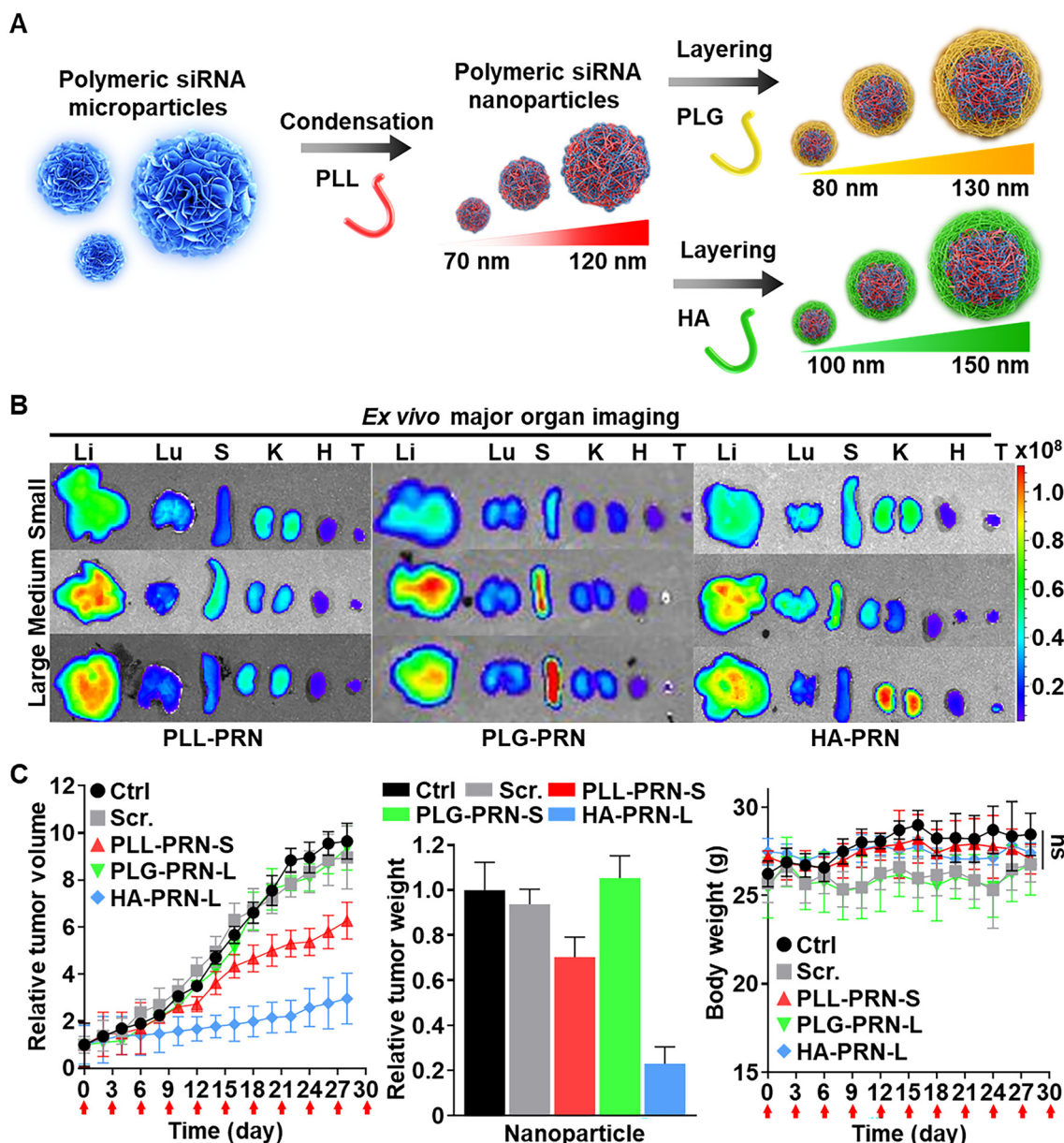


Fig. 6 Size/surface chemistry-tuned polymeric RNA nanostructures (PRN) for *in vivo* systemic delivery with tumor-targeted delivery. (A) Scheme for synthesis of size/surface chemistry-tuned PRN. (B) *Ex vivo* biodistribution and (C) *in vivo* antitumor effect of size/surface chemistry-tuned PRN. Reproduced with permission from ref. 18 Copyright 2024, American Chemical Society. PLL, poly-L-lysine; PLG, poly-L-glutamate; HA, hyaluronic acid; Ctrl, control; Scr., scrambled; PLL-PRN-S, small-sized PLL-layered PRN; PLG-PRN-S, small-sized PLG-layered PRN; HA-PRN-L, large-sized HA-layered PRN.

active targeting. Compared with PLG-PRN-S and PLL-PRN-S, HA-PRN-L achieved 3.8- and 2.9-fold higher tumor accumulation, respectively. These nanoparticles also promoted efficient endosomal escape *via* the proton sponge effect and induced potent PLK1 knockdown, resulting in approximately 80% tumor reduction in mouse models without observable toxicity (Fig. 6C).

Taken together, these studies demonstrate the versatility of RCR based nanostructures for building ligand-targeted and intracellularly targeted delivery platforms. Their high loading capacity, structural tunability, and compatibility with diverse therapeutic cargos make them promising candidates for application in next generation precision medicine. Further exploration of ligand combinations, intracellular trafficking mechanisms, and *in vivo* optimization is essential to advance these systems toward preclinical translation.

4.3. Stimulus responsive delivery

Because of the dynamic nature of nucleic acids and their sequence-mediated functionalities, the evolution of RCR based nucleic acid nanostructures has opened new avenues for stimuli responsive drug delivery. DNA and RNA nanostructures can be engineered to detect and respond to specific internal or external triggers, leading to the controlled release of therapeutic cargo. These systems integrate structural programmability with molecular sensitivity, enabling precise control over cargo release in response to cues, such as enzymatic activity, pH, redox gradients, or even light.

A conformational change of polymeric nucleic acid nanostructures can induce rapid release of their loaded drug. Zhang *et al.* demonstrated that model protein drugs can be loaded in polymeric DNA nanostructures and released by conformational change *via* DNA–DNA complementary binding or DNA aptamer–ligand interaction.⁸⁵ Proteins were encapsulated in polymeric DNA nanostructures *via* one-pot RCA and three types of aptamers (adenosine triphosphate, platelet-derived growth factor, and toxin B) induced rapid release of loaded proteins. Further, protein release by complementary binding was highly dependent on the sequence length and the number of matching sequences. This structural change leads to the rapid disintegration of the scaffold and immediate release of encapsulated proteins, occurring within minutes rather than hours. This mechanism is a modular strategy highly adaptable to various biological targets.

Given that the i-motif sequence can induce DOX intercalation as well as pH responsive release, Nam *et al.* incorporated i-motif and AS1411 sequences into polymeric DNA nanostructures for tumor-specific targeting and stimulus responsive drug release (Fig. 7A).²⁵ The crystallinity of ultrasoft, self-supporting polymeric DNA networks (pDNets) was tuned by controlling MgPPi–DNA ratios during RCA to regulate nanoporosity, mechanical properties, and drug localization. The pDNets exhibited a 9-fold range in mechanical properties, optimizing injectability and structural stability. Furthermore, incorporation of functional DNA sequences conferred pH responsive drug release and aptamer-mediated cancer cell targeting.

Moreover, pDNets functionalized with the AS1411 aptamer and i-motif structures enable controlled cell attachment and localized DOX release within the acidic TME, without inducing significant toxicity (Fig. 7B). This functionality was further validated *in vivo*, where pDNets with lower crystallinity achieved superior therapeutic efficacy, likely due to enhanced sequence accessibility and reduced steric hindrance associated with decreased crystallinity (Fig. 7C). This one pot enzymatic polymerization approach offers precise control over mechanical and physicochemical properties for localized, stimuli responsive drug delivery using RCA derived DNA networks.

Although rod-shaped nanoparticles can enhance intracellular delivery efficiency, strategies to decorate them with additional functionalities are lacking. To address this, Lee *et al.* developed DOX-loaded polymeric DNA-decorated CNCs (pDCs) *via* RCA and electrostatic interaction to provide functionalities for stimuli responsive and target-specific delivery (Fig. 8A).⁶⁶ This system leverages AS1411 aptamer and i-motif structures for aptamer-mediated cancer targeting and TME pH sensitive DOX release by DNA structural disruption. The rod shape of CNCs enabled efficient delivery to cancer cells and the density of functionalized polymeric DNA for pDCs was tuned for controlled biological function and stability (Fig. 8B). This strategy provides a biocompatible and modular framework for responsive drug delivery using nucleic acid based hybrids.

Complexing nucleic acids with upconversion nanoparticles (UCNP) has been utilized for synergistic therapeutics as UCNPs convert longer wavelength light to shorter wavelength light. Song *et al.* decorated UCNPs with a multifunctional polymeric DNA (UCND) *via* RCA, integrating gene editing and ROS amplification for synergistic photodynamic therapy (PDT).⁸⁶ Polymeric DNA from RCA was designed with sgRNA recognition and G-quadruplex sequence to load Cas9 RNP, hemin, and protoporphyrin (PP). The intracellular delivered UCND released Cas9 RNP by cleavage of DNA–RNA complex *via* RNase H, overexpressed in cancer cells, resulting in knockout of nuclear factor E2 related factor 2 (Nrf2) to improve the sensitivity to ROS. In addition, UCND converted NIR irradiation to short wavelength irradiation, resulting in PP activation to generate ROS. Hemin induced H₂O₂ decomposition into O₂, elevating tumor hypoxia and ¹O₂ production. This approach significantly enhanced PDT efficacy in a breast cancer mouse model.

To avoid unwanted drug release in normal cells, strategies for cancer-specific targeting and release have been attempted. Guo *et al.* designed a redox responsive RNA delivery system using pompom-like nanostructures synthesized by RCT.⁸⁷ Long anti-miRNA-21 RNA strands were transcribed from circular DNA templates and condensed into nanoparticles using the GSH-sensitive cationic polymer polyethyleneimine. Furthermore, it was modified with dehydroascorbic acid to target glucose transfer 1 (GLUT-1), which is overexpressed on cancer cell membranes. Once internalized by cancer cells, elevated intracellular GSH levels trigger polymer degradation, rapidly disassembling the structure and releasing anti-miRNA-21 to suppress oncogenic pathways.

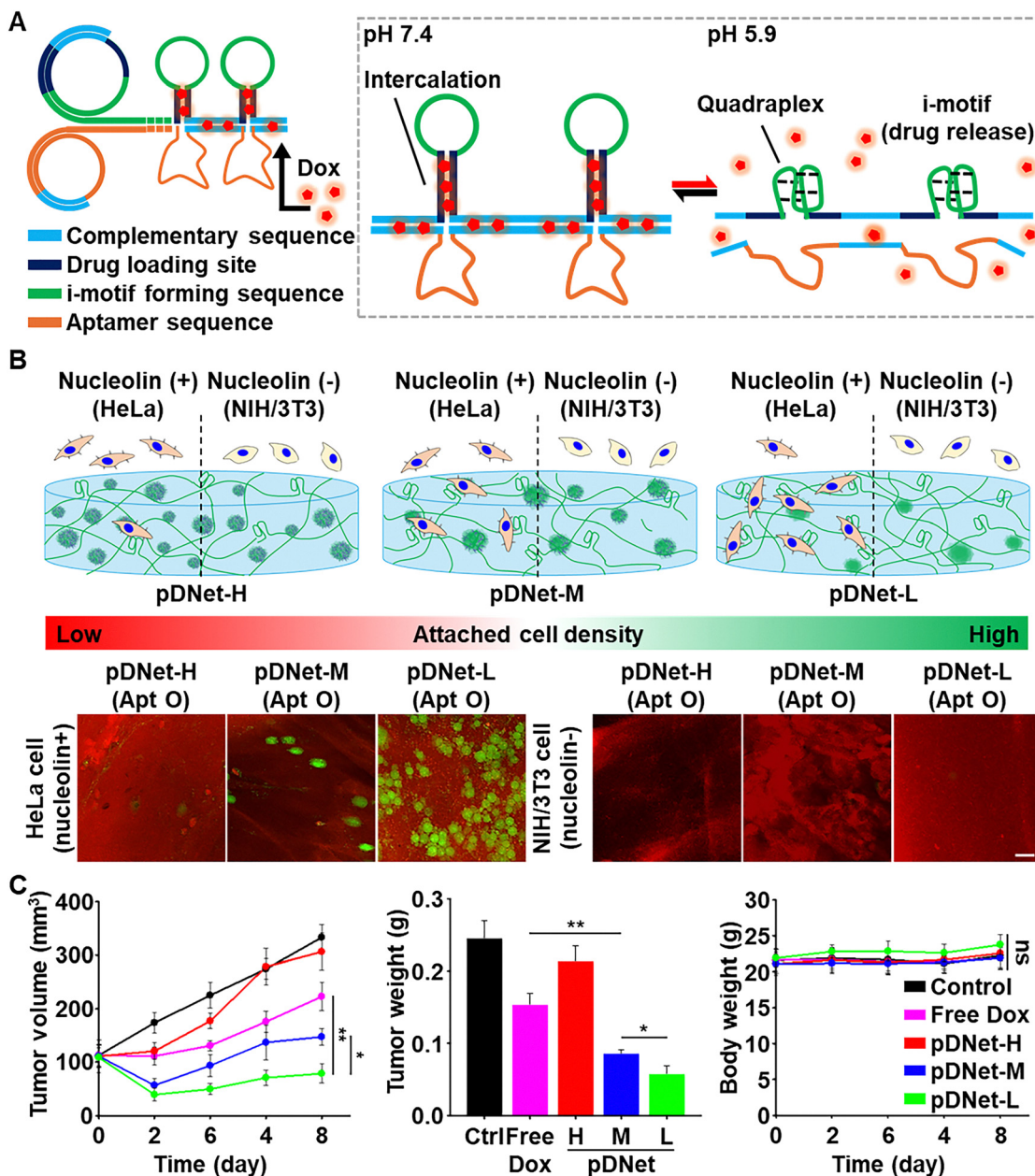


Fig. 7 Crystallinity-tuned ultrasoft polymeric DNA networks (pDNets) for targeted and controlled release of anticancer drugs. (A) Schematic for pH-stimulus release of i-motif sequence in pDNets. (B) Schematic and confocal laser scanning microscope images for targeted and controlled cancer cell attachment of AS1411 sequence in pDNets. (C) *In vivo* antitumor effect of pDNets with varied crystallinity. Reproduced with permission from ref. 25 Copyright 2023, Elsevier Ltd. Dox, doxorubicin; pDNet-H, polymeric DNA network-high crystallinity; pDNet-M, polymeric DNA network-medium crystallinity; pDNet-L, polymeric DNA network-low crystallinity; Apt, aptamer.

Altogether, these RCR based delivery systems demonstrate the diversity and adaptability of nucleic acid nanostructures in response to biologically and externally relevant triggers. Through enzyme activation, pH sensitivity, redox gradients, molecular recognition, or photothermal heating, these platforms provide programmable and modular mechanisms for drug release. Their versatility in incorporating ligand targeting, structural tuning, and functional responsiveness underscores their promise for developing precision next-generation therapeutics.

5. Summary and perspective

RCR based nucleic acid nanostructures have been tailored for a wide range of drug delivery applications, including gene regulation, immunostimulation, catalysis, targeting, and stimuli responsiveness, owing to their excellent biocompatibility and intrinsic biological functions. By employing multiple types of circular DNA templates, these nanostructures can be simultaneously endowed with diverse biological functionalities. Their physicochemical properties can be finely controlled using

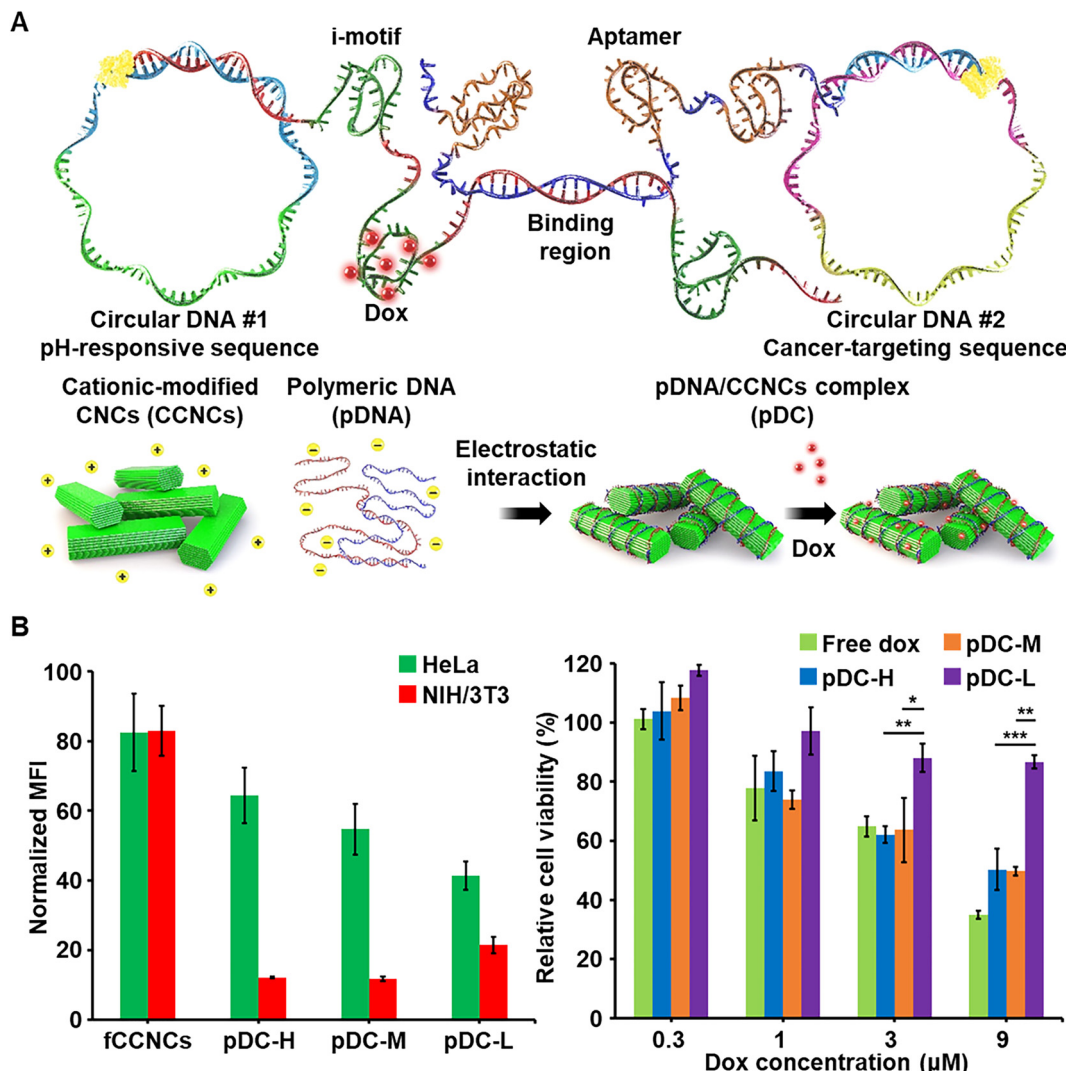


Fig. 8 Polymeric DNA-decorated cellulose nanocrystals (CNCs) for targeted and stimuli responsive drug delivery. (A) Scheme for synthesis of polymeric DNA nanostructure-decorated cellulose nanocrystals. (B) Intracellular delivery and apoptotic effect in HeLa cells of polymeric DNA nanostructure-decorated cellulose nanocrystals. Reproduced with permission from ref. 66 Copyright 2024, Elsevier Ltd. Dox, doxorubicin; MFI, mean fluorescence intensity; fCCNCs, fluorescent cationic CNCs; pDC-H, pDC with high CCNCs/pDNA ratio; pDC-M, pDC with medium CCNCs/pDNA ratio; pDC-L, pDC with low CCNCs/pDNA ratio.

various engineering approaches. The reaction conditions influence not only the length of the nucleic acids as well as the size, crystallinity, and density of the resulting organic–inorganic hybrid particles. Meanwhile, integration with functional materials such as biopolymers and metal ions allows control over the size, morphology, structure, surface charge, and functionality of these nanostructures. Collectively, these nanostructures have enabled promising outcomes in advanced drug delivery strategies, including passive targeting, active targeting, and stimulus responsive systems.

Despite these advantages, several challenges remain before RCR based nucleic acid nanostructures are clinically translated. (1) The applications of RCR based nucleic acid nanostructures are often limited by their inherently low stability. Nucleic acids are susceptible to degradation by nucleases under physiological conditions and are unstable at high temperatures or extreme

pH conditions of chemical modifications to functionalize nanostructures. These issues can be mitigated by incorporating functional materials or utilizing pre-chemically modified nucleotides to improve stability and functionalization. (2) Although RCR enables isothermal enzymatic amplification of ultra-long nucleic acid nanostructures with programmable sequences, its practical utility is hampered by high production costs, error-prone replication, and the sensitivity of enzymatic efficiency to storage and reaction conditions. Scalable manufacturing, real-time reaction monitoring, and efficient purification systems are necessary to overcome these limitations. (3) Current applications of RCR based nanostructures for programmable drug delivery are restricted to only a few biological activities. This scope should be broadened by diversifying the RCR strategies, such as designing circular DNA templates with varied functionalities, employing multiple types of circular

DNA templates, and incorporating additional functional materials to construct more versatile drug delivery platforms and therapeutic modalities. (4) Although preclinical models have shown promising results, comprehensive *in vivo* and clinical data regarding the therapeutic efficacy and safety of RCR based nucleic acid nanostructures remain limited. The potential immunogenicity of ultra-long concatemeric sequences and the toxicity of hybrid materials, such as biopolymers or lipids, must be rigorously evaluated in clinical models. Moreover, detailed pharmacokinetic studies on the physicochemical properties of nanostructures are essential to overcome biological barriers and advance clinical applications.

In summary, RCR based engineering strategies are powerful approaches for constructing polymeric nucleic acid nanostructures with high programmability and therapeutic potential. With continued progress in nucleic acid nanotechnology and biomaterial research, these systems can play an increasingly pivotal role in the future of programmable drug delivery and broader biomedical innovations.

Author contributions

K. Y. and Y. H. R. contributed to the project conceptualization. K. Y., K. N., K. H. P., H. K. S., and Y. K. prepared the original draft. Y. H. R. revised and edited the manuscript. K. Y. and H. K. S. visualized the figures. Y. H. R. supervised the project. All authors approved the final version of the manuscript.

Conflicts of interest

The authors declare no conflict of interest.

Data availability

No primary research results, software or code have been included and no new data were generated or analysed as part of this review.

Acknowledgements

This research was supported by the National Research Foundation (NRF) grant funded by the Korean government (MSIT) (No. RS-2025-16071710, RS-2024-00360849, and RS-2025-00517193). The work was also supported in part by Brain Korea 21 (BK21) FOUR program.

References

- 1 R. R. Breaker, *Nature*, 2004, **432**(7019), 838–845.
- 2 N. C. Seeman and H. F. Sleiman, *Nat. Rev. Mater.*, 2017, **3**(1), 1–23.
- 3 P. Guo, *Nat. Nanotechnol.*, 2010, **5**, 833–842.
- 4 Y. H. Roh, R. C. Ruiz, S. Peng, J. B. Lee and D. Luo, *Chem. Soc. Rev.*, 2011, **40**(12), 5730–5744.
- 5 T. Kim, K. Nam, Y. M. Kim, K. Yang and Y. H. Roh, *ACS Nano*, 2021, **15**(2), 1942–1951.
- 6 C. Yang, X. Wu, J. Liu and B. Ding, *Nanoscale*, 2022, **14**(48), 17862–17870.
- 7 A. Fire and S. Q. Xu, *Proc. Natl. Acad. Sci. U. S. A.*, 1995, **92**(10), 4641–4645.
- 8 S. L. Daubendiek, K. Ryan and E. T. Kool, *J. Am. Chem. Soc.*, 1995, **117**(29), 7818–7819.
- 9 M. Du, J. Liu, G. Teng, F. Shi, Y. Dong and F. Li, *Chin. J. Chem.*, 2025, **43**(13), 1587–1604.
- 10 S. Yue, Y. Li, Z. Qiao, W. Song and S. Bi, *Trends Biotechnol.*, 2021, **39**(11), 1160–1172.
- 11 X. Ma, Y. Zhang, K. Huang, L. Zhu and W. Xu, *Biomaterials*, 2023, **301**, 122241.
- 12 A. M. Vargason, A. C. Anselmo and S. Mitragotri, *Nat. Biomed. Eng.*, 2021, **5**(9), 951–967.
- 13 S. Wilhelm, A. J. Tavares, Q. Dai, S. Ohta, J. Audet, H. F. Dvorak and W. C. Chan, *Nat. Rev. Mater.*, 2016, **1**(5), 1–12.
- 14 A. Verma and F. Stellacci, *Small*, 2010, **6**(1), 12–21.
- 15 J. Li and D. J. Mooney, *Nat. Rev. Mater.*, 2016, **1**(12), 1–17.
- 16 K. E. Shopsowitz, C. Wu, G. Liu, E. C. Dreden and P. T. Hammond, *Nucleic Acids Res.*, 2016, **44**(2), 545–557.
- 17 H. Kim, Y. Park and J. B. Lee, *Sci. Rep.*, 2015, **5**(1), 12737.
- 18 T. Kim, H. S. Han, K. Yang, Y. M. Kim, K. Nam, K. H. Park, S. Y. Choi, H. W. Park, K. Y. Choi and Y. H. Roh, *ACS Nano*, 2024, **18**(11), 7972–7988.
- 19 K. Nam, T. Kim, Y. M. Kim, K. Yang, D. Choe, L. B. Mensah, K. Y. Choi and Y. H. Roh, *Chem. Commun.*, 2019, **55**(34), 4905–4908.
- 20 H. Kim, J. Jeong, D. Kim, G. Kwak, S. H. Kim and J. B. Lee, *Adv. Sci.*, 2017, **4**(8), 1600523.
- 21 Y. R. Baker, J. Chen, J. Brown, A. H. El-Sagheer, P. Wiseman, E. Johnson, P. Goddard and T. Brown, *Nucleic Acids Res.*, 2018, **46**(15), 7495–7505.
- 22 J. S. Lee, H. Kim, C. Jo, J. Jeong, J. Ko, S. Han, M. S. Lee, H. Lee, J. W. Han, J. Lee and J. B. Lee, *Adv. Funct. Mater.*, 2017, **27**(45), 1704213.
- 23 D. Kim, S. J. Kim, J. Jeong, S. Han, H. Kim, S. Lee, I. Choi, J. Hong, J. Jin and J. B. Lee, *ACS Nano*, 2024, **18**(2), 1744–1755.
- 24 Y. M. Kim, K. Nam, H. Y. Kim, K. Yang, B. S. Kim, D. Luo and Y. H. Roh, *Small Methods*, 2024, 2401881.
- 25 K. Nam, Y. M. Kim, I. Choi, H. S. Han, T. Kim, K. Y. Choi and Y. H. Roh, *J. Controlled Release*, 2023, **355**, 7–17.
- 26 H. Zhao, X. Yuan, J. Yu, Y. Huang, C. Shao, F. Xiao, L. Lin, Y. Li and L. Tian, *ACS Appl. Mater. Interfaces*, 2018, **10**(18), 15418–15427.
- 27 D. Han, Y. Park, H. Kim and J. B. Lee, *Nat. Commun.*, 2014, **5**(1), 4367.
- 28 J. K. Lam, M. Y. Chow, Y. Zhang and S. W. Leung, *Mol. Ther. Nucl. Acids*, 2015, **4**, e252.
- 29 J. B. Lee, J. Hong, D. K. Bonner, Z. Poon and P. T. Hammond, *Nat. Mater.*, 2012, **11**(4), 316–322.
- 30 K. E. Shopsowitz, Y. H. Roh, Z. J. Deng, S. W. Morton and P. T. Hammond, *Small*, 2014, **10**(8), 1623–1633.

31 Y. H. Roh, J. Z. Deng, E. C. Dreaden, J. H. Park, D. S. Yun, K. E. Shopsowitz and P. T. Hammond, *Angew. Chem., Int. Ed.*, 2016, **55**(10), 3347–3351.

32 T. Kim, H. N. Hyun, R. Heo, K. Nam, K. Yang, Y. M. Kim, Y. S. Lee, J. Y. An, J. H. Park, K. Y. Choi and Y. H. Roh, *Chem. Commun.*, 2020, **56**(49), 6624–6627.

33 E. Kwak, T. Kim, K. Yang, Y. M. Kim, H. S. Han, K. H. Park, K. Y. Choi and Y. H. Roh, *Biomacromolecules*, 2022, **23**(6), 2255–2263.

34 C. Wu, K. E. Shopsowitz and P. T. Hammond, *Mol. Ther.*, 2016, **24**(6), 1070–1077.

35 G. Tang, *Trends Biochem. Sci.*, 2015, **30**(2), 106–114.

36 H. Kim, E. Lee, Y. Y. Kang, J. Song, H. Mok and J. B. Lee, *Adv. Biosyst.*, 2018, **2**(2), 1700158.

37 S. T. Crooke, B. F. Baker, R. M. Crooke and X. H. Liang, *Nat. Rev. Drug Discovery*, 2021, **20**(6), 427–453.

38 Y. H. Roh, J. B. Lee, K. E. Shopsowitz, E. C. Dreaden, S. W. Morton, Z. Poon, J. Hong, I. Yamin, D. K. Bonner and P. T. Hammond, *ACS Nano*, 2014, **8**(10), 9767–9780.

39 L. C. Li, S. T. Okino, H. Zhao, D. Pookot, R. F. Place, S. Urakami, H. Enokida and R. Dahiya, *Proc. Natl. Acad. Sci. U. S. A.*, 2006, **103**(46), 17337–17342.

40 T. Wang, S. Hong, Y. Luo, H. Lv, Y. Zhang and R. Pei, *ACS Appl. Bio Mater.*, 2019, **2**(11), 4737–4746.

41 Y. Shi, M. Shi, Y. Wang and J. You, *Signal Transduction Targeted Ther.*, 2024, **9**(1), 322.

42 Y. Tang, X. Liao, C. Wang, Y. Liu, J. Pan, Y. Tian, Z. Teng and G. Lu, *J. Colloid Interface Sci.*, 2021, **603**, 191–198.

43 L. Z. Kong, S. M. Kim, C. Wang, S. Y. Lee, S. C. Oh, S. Lee, S. Jo and T. D. Kim, *Exp. Mol. Med.*, 2023, **55**(11), 2320–2331.

44 G. Zhu, L. Mei, H. D. Vishwasrao, O. Jacobson, Z. Wang, Y. Liu, B. C. Yung, X. Fu, A. Jin, G. Niu, Q. Wang, F. Zhang, H. Shroff and X. Chen, *Nat. Commun.*, 2017, **8**(1), 1482.

45 Y. Huang, X. Liu, J. Zhu, Z. Chen, L. Yu, X. Huang, C. Dong, J. Li, H. Zhou, Y. Yang and W. Tan, *J. Am. Chem. Soc.*, 2024, **146**(20), 13805–13816.

46 F. Li, N. Song, Y. Dong, S. Li, L. Li, Y. Liu, Z. Li and D. Yang, *Angew. Chem., Int. Ed.*, 2022, **61**(9), e202116569.

47 C. Yao, H. Qi, X. Jia, Y. Xu, Z. Tong, Z. Gu and D. Yang, *Angew. Chem., Int. Ed.*, 2022, **61**(6), e202113619.

48 R. Micura and C. Höbartner, *Chem. Soc. Rev.*, 2020, **49**(20), 7331–7353.

49 D. L. Jasinski, D. W. Binzel and P. Guo, *ACS Nano*, 2019, **13**(4), 4603–4612.

50 D. Agudelo, P. Bourassa, G. Bérubé and H. A. Tajmir-Riahi, *Int. J. Biol. Macromol.*, 2014, **66**, 144–150.

51 L. R. Rutledge, L. S. Campbell-Verduyn and S. D. Wetmore, *Chem. Phys. Lett.*, 2007, **444**(1–3), 167–175.

52 L. Zhang, R. Abdullah, X. Hu, H. Bai, H. Fan, L. He, H. Liang, J. Zou, Y. Liu, Y. Sun, X. Zhang and W. Tan, *J. Am. Chem. Soc.*, 2019, **141**(10), 4282–4290.

53 C. Yao, J. Tang, C. Zhu, S. Yang, H. Tang, L. Dong, C. Zhang, Q. Tang, P. Liu and D. Yang, *Nano Today*, 2022, **42**, 101352.

54 H. Zhao, L. Li, F. Li, C. Liu, M. Huang, J. Li, F. Gao, X. Ruan and D. Yang, *Adv. Mater.*, 2022, **34**(13), 2109920.

55 H. Zhao, Z. Zhang, D. Zuo, L. Li, F. Li and D. Yang, *Nano Lett.*, 2021, **21**(12), 5377–5385.

56 J. A. Holland and D. W. Hoffman, *Nucleic Acids Res.*, 1996, **24**(14), 2841–2848.

57 L. Ding, J. Li, C. Wu, F. Yan, X. Li and S. Zhang, *J. Mater. Chem. B*, 2020, **8**(16), 3527–3533.

58 J. S. Ha, J. S. Lee, J. Jeong, H. Kim, J. Byun, S. A. Kim, H. J. Lee, H. S. Chung, J. B. Lee and D. R. Ahn, *J. Controlled Release*, 2017, **250**, 27–35.

59 Z. Zhang, D. Xu, J. Wang, R. Zhang, H. Du, T. Zhou, X. Wang and F. Wang, *Biomacromolecules*, 2022, **24**(1), 439–448.

60 T. Hermann and D. J. Patel, *Science*, 2000, **287**(5454), 820–825.

61 B. T. Tran, J. Kim and D. R. Ahn, *Nanoscale*, 2020, **12**(45), 22945–22951.

62 X. Chen, X. He, R. Gao, X. Lan, L. Zhu, K. Chen, Y. Hu, K. Huang and W. Xu, *ACS Nano*, 2021, **16**(1), 1036–1050.

63 R. Zhang, Z. Lv, L. Chang, J. Wang, J. Tang, Z. Wang, S. Li, J. Guo, C. Yao and D. Yang, *Adv. Funct. Mater.*, 2024, **34**(32), 2401563.

64 J. Lee, Q. V. Le, G. Yang and Y. K. Oh, *Biomaterials*, 2019, **218**, 119359.

65 H. A. Assi, M. Garavís, C. González and M. J. Damha, *Nucleic Acids Res.*, 2018, **46**(16), 8038–8056.

66 Y. Lee, K. Nam, Y. M. Kim, K. Yang, Y. Kim, J. W. Oh and Y. H. Roh, *Carbohydr. Polym.*, 2024, **340**, 122270.

67 N. Srinivas, T. E. Ouldridge, P. Šulc, J. M. Schaeffer, B. Yurke, A. A. Louis, J. P. K. Doye and E. Winfree, *Nucleic Acids Res.*, 2013, **41**(22), 10641–10658.

68 W. Sun, W. Ji, J. M. Hall, Q. Hu, C. Wang, C. L. Beisel and Z. Gu, *Angew. Chem., Int. Ed.*, 2015, **127**(41), 12197–12201.

69 J. Shi, X. Yang, Y. Li, D. Wang, W. Liu, Z. Zhang, J. Liu and K. Zhang, *Biomaterials*, 2020, **256**, 120221.

70 E. Kim, S. Agarwal, N. Kim, F. S. Hage, V. Leonardo, A. Gelmi and M. M. Stevens, *ACS Nano*, 2019, **13**(3), 2888–2900.

71 D. Liu, S. L. Daubendiek, M. A. Zillman, K. Ryan and E. T. Kool, *J. Am. Chem. Soc.*, 1996, **118**(7), 1587–1594.

72 D. Mao, W. Li, X. Liu, J. Chen, D. Wei, L. Luo, Q. Yuan, Y. Yang, X. Zhu and W. Tan, *Chem*, 2025, **11**, 2.

73 Y. Lv, R. Hu, G. Zhu, X. Zhang, L. Mei, Q. Liu, L. Qiu, C. Wu and W. Tan, *Nat. Protoc.*, 2015, **10**(10), 1508–1524.

74 Y. Wang, E. Kim, Y. Lin, N. Kim, W. Kit-Anan, S. Gopal, S. Agarwal, P. D. Howes and M. M. Stevens, *ACS Appl. Mater. Interfaces*, 2019, **11**(26), 22932–22940.

75 Y. R. Baker, L. Yuan, J. Chen, R. Belle, R. Carlisle, A. H. El-Sagheer and T. Brown, *Nucleic Acids Res.*, 2021, **49**(16), 9042–9052.

76 C. Castro, E. D. Smidansky, J. J. Arnold, K. R. Maksimchuk, I. Moustafa, A. Uchida, M. Götte, W. Konigsberg and C. E. Cameron, Nucleic acid polymerases use a general acid for nucleotidyl transfer, *Nat. Struct. Mol. Biol.*, 2009, **16**(2), 212–218.

77 J. Chen, Y. R. Baker, A. Brown, A. H. El-Sagheer and T. Brown, *Chem. Sci.*, 2018, **9**(42), 8110–8120.

78 J. Li, J. Yu, Y. Huang, H. Zhao and L. Tian, *ACS Appl. Mater. Interfaces*, 2018, **10**(31), 26075–26083.

79 J. B. Lee, S. Peng, D. Yang, Y. H. Roh, H. Funabashi, N. Park, E. J. Rice, L. Chen, R. Long, M. Wu and D. Luo, *Nat. Nanotechnol.*, 2012, **7**(12), 816–820.

80 C. Yao, H. Tang, W. Wu, J. Tang, W. Guo, D. Luo and D. Yang, *J. Am. Chem. Soc.*, 2020, **142**(7), 3422–3429.

81 H. Kim, Y. K. Lee, K. H. Han, H. Jeon, I. H. Jeong, S. Y. Kim, J. B. Lee and P. C. Lee, *Biomaterials*, 2020, **230**, 119630.

82 Y. M. Kim, Y. S. Lee, T. Kim, K. Yang, K. Nam, D. Choe and Y. H. Roh, *Carbohydr. Polym.*, 2020, **247**, 116684.

83 X. Xu, S. Li, W. Yu, S. Yao, H. Fan and Z. Gou, *Angew. Chem., Int. Ed.*, 2024, **136**(10), e202318544.

84 S. Han, W. Yoo, O. Carton, J. Joo and E. J. Kwon, *Small*, 2025, **21**(10), 2405806.

85 Y. Zhang, Q. Zhang, F. Cheng, Y. Chang, M. Liu and Y. Li, *Chem. Sci.*, 2021, **12**(24), 8282–8287.

86 N. Song, X. Fan, X. Gou, J. Tang, H. Li, R. Tao, F. Li, J. Li, D. Yang, C. Yao and P. Liu, *Adv. Mater.*, 2024, **36**(15), 2309534.

87 Q. Guo, C. Li, W. Zhou, X. Chen, Y. Zhang, Y. Lu, Y. Zhang, Q. Chen, D. Liang, T. Sun and C. Jiang, *Acta Pharm. Sin. B*, 2019, **9**(4), 832–842.